GDAŃSKI UNIWERSYTET MEDYCZNY

Wybrane markery neuroobrazowe i biochemiczne w szacowaniu rokowania tkankowego, w tym ryzyka śródczaszkowych powikłań krwotocznych, u pacjentów z ostrym udarem niedokrwiennym mózgu leczonych trombolitycznie

Selected neuroimaging and biochemical parameters combined for prospective assessment of tissue outcome and the risk of rtPA-associated intracerebral hemorrhage in patients with acute ischemic stroke

Bartosz Jabłoński

ROZPRAWA NA STOPIEŃ DOKTORA NAUK MEDYCZNYCH

PROMOTOR

Prof. dr hab. n. med. Bartosz Karaszewski

KLINIKA NEUROLOGII DOROSŁYCH
GDAŃSKI UNIWERSYTET MEDYCZNY

GDAŃSK 2022

Pragnę złożyć serdeczne podziękowania mojemu Promotorowi, Mentorowi i Przewodnikowi w świecie nauki, prof. dr. hab. n. med. Bartoszowi Karaszewskiemu, za inspirację, wsparcie merytoryczne i przygotowanie niniejszej dysertacji, a także za cierpliwość i wszelką bezinteresowną pomoc.

Pracę dedykuję mojej żonie Marcie i synkowi Ignacemu.
Dziękuję Wam, że jesteście przy mnie, wspieracie mnie i dodajecie sił.

Dziękuję Rodzicom – za to, że zawsze we mnie wierzycie.

SPIS TREŚCI

WYKAZ PUBLIKACJI WCHODZĄCYCH W SKŁAD ROZPRAWY DOKTORSKIEJ

1. Karaszewski B, Jabłoński B, Żukowicz W. The salvageable brain in acute ischemic stroke. The concept of a reverse mismatch: a mini-review. Metab Brain Dis. 2020 Feb;35(2):237-240.
   doi: 10.1007/s11011-019-00517-x.
   Punktacja IF: 3.584
   Punktacja MEiN: 70.000

2. Jabłoński B, Gójska-Grymajło A, Ossowska D, Szurowska E, Wyszomirski A, Rojek B, Karaszewski B. New remote cerebral microbleeds on T2*-Weighted Echo Planar Magnetic Resonance Imaging after intravenous thrombolysis for acute ischemic stroke. Front Neurol. 2022; ;12:744701.
   Published 2022 Feb 15.
   doi:10.3389/fneur.2021.744701
   Punktacja IF: 4.003
   Punktacja MEiN: 100.000

3. Karaszewski B, Gójska-Grymajło A, Czaplewska P, Jabłoński B, Lewandowska AE, Ossowska D, Wyszomirski A, Hałas M, Szurowska E. SWATH-MS for prospective identification of protein blood biomarkers of rtPA-associated intracranial hemorrhage in acute ischemic stroke: a pilot study. Sci Rep. 2021 Sep 21;11(1):18765.
   doi: 10.1038/s41598-021-97710-9.
   Punktacja IF: 4.380
   Punktacja MEiN: 140.000

Całkowita punktacja IF: 11.967
Całkowita punktacja MEiN: 310.000

WYKAZ STOSOWANYCH SKRÓTÓW

AIS	*acute ischemic stroke*	ostry udar niedokrwienny mózgu (OUNM)
AHA/ASA	*American Heart Association/American Stroke Association*	Amerykańskie Towarzystwo Kardiologiczne/Udarowe
CBF	*cerebral blood flow*	mózgowy przepływ krwi
CBV	*cerebral blood volume*	mózgowa objętość krwi
CE	*cardioembolic stroke*	udar sercowo-zatorowy
CMBs	*cerebral microbleeds*	mikrokrwawienia mózgowe
CTA	*computed tomography angiography*	angiografia tomografii komputerowej
CTP	*computed tomography perfusion*	perfuzja tomografii komputerowej
DALY	*disability adjusted life-years*	liczba lat utraconych wskutek choroby - śmierci lub trwałej niepełnosprawności
DTI	*diffusion tensor imaging*	obrazowanie tensora dyfuzji
DWI	*diffusion-weighted imaging*	obrazowanie dyfuzyjne
EBM	*evidence based medicine*	medycyna oparta na dowodach
ECASS-II	*The European Cooperative Acute Stroke Study scale*	-
EPI	*echo-planar imaging*	sekwencja echa planarnego
ESO	*European Stroke Organisation*	Europejska Organizacja Udarowa
FLAIR	*fluid-attenuated inversion recovery*	sekwencja wygaszenia płynu – odzysku inwersji
GBD 2019	*Global Burden of Disease 2019*	Globalne Obciążenie Chorobami 2019
GRE	*gradient recalled echo*	sekwencja echa gradientowego
HAS-BLED	-	Skala Krwawień Birmingham
HI 1, 2	*hemorrhagic infarction type 1, 2*	zawał krwotoczny typu 1, 2
IVT	*intravenous thrombolysis*	tromboliza dożylna
LVD	*large-vessel disease*	choroba dużych naczyń
LVO	*large vessel occlusion*	zamknięcie dużego naczynia
MRI	*magnetic resonance imaging*	rezonans magnetyczny
MTT	*mean transit time*	średni czas przejścia
NFZ	*Polish National Health Fund*	Narodowy Fundusz Zdrowia
NIHSS	*National Institutes of Health Stroke Scale*	Skala Oceny Udaru Narodowych Instytutów Zdrowia
ncCT	*non-contrast computed tomography*	tomografia komputerowa bez kontrastu
OAC	*oral anticoagulant*	doustny lek przeciwkrzepliwy

PH 1, 2	*parenchymal hematoma type 1, 2*	krwiak śródmiąższowy typu 1, 2
rICH	*remote-intracerebral hemorrhage*	krwawienie śródmózgowe anatomicznie odległe
rtPA	*recombinant tissue plasminogen activator*	rekombinowany tkankowy aktywator plazminogenu
sICH	*symptomatic intracerebral hemorrhage*	objawowe krwawienie śródmózgowe
SITS-MOST	*The Safe Implementation of Thrombolysis in Stroke-Monitoring Study*	-
SVD	*small vessel disease*	choroba małych naczyń mózgowych
SWATH-MS	*Sequential Window Acquisition of All Theoretical Mass Spectra*	
SWI	*susceptibility weighted imaging*	sekwencja podatności magnetycznej
TOAST	*Trial of Org 10172 in Acute Stroke Treatment*	klasyfikacja etiologiczna udaru mózgu
TSE	*turbo-spin echo*	sekwencja echa spinowego
UE	*stroke of unknown etiology*	udar mózgu o nieustalonej etiologii
WHO	*World Health Organization*	Światowa Organizacja Zdrowia

WSTĘP

Udar mózgu (UM) jest najczęstszą przyczyną trwałej niepełnosprawności ludzi dorosłych na świecie i drugą przyczyną zgonów. Według danych Światowej Organizacji Zdrowia (WHO, World Health Organization) w 2019 odnotowano 12.2 mln zachorowań, 6.55 mln zgonów (w tym 2.7 mln z powodu udaru niedokrwiennego mózgu, UNM) i łącznie 143 mln lat utraconych wskutek choroby - śmierci lub trwałej niepełnosprawności (DALYs, disability adjusted life-years)[GBD 2019 Stroke Collaborators]. Około 85% wszystkich UM stanowią udary niedokrwienne mózgu (UNM). Zgodnie z danymi Narodowego Funduszu Zdrowia (NFZ)[NFZ o zdrowiu. Udar niedokrwienny mózgu. 2019], rocznie z powodu UNM w Polsce hospitalizowanych jest ponad 70 tys. osób przy czym w latach 2013-2018 odnotowano spadek liczby pacjentów, którzy byli hospitalizowani z powodu UNM o 7.6% - z 75.7 tys. do 70.7 tys.

Terapie rekanalizacyjno-reperfuzyjne ostrego UNM (OUNM), w łączności z niespecyficznymi metodami postępowania, znacząco poprawiły rokowanie w tej grupie pacjentów. Leczenie trombolityczne dożylne (IVT, intravenous thrombolysis) z wykorzystaniem rekombinowanego tkankowego aktywatora plazminogenu (rtPA, recombinant tissue plasminogen activator) – częściej alteplazy, rzadziej tenekteplazy (wytyczne postępowania AHA/ASA, American Heart Association/American Stroke Association oraz ESO, European Stroke Organisation, wskazują na korzyści z wyboru tenekteplazy w przypadku OUNM z zamknięciem dużej tętnicy, LVO, large vessel occlusion), a także trombektomia mechaniczna są podstawowymi metodami terapii przyczynowej – reperfuzyjnej pacjentów z OUNM. Według zasad medycyny opartej na faktach (EBM, evidence based medicine) skuteczność tych metod cechuje najwyższy poziom dowodów naukowych, zaś w standardach postępowania mają najwyższą klasę rekomendacji eksperckich[Emberson et al. 2014; Goyal et al. 2016]. Wyjątek stanowi OUNM w przebiegu choroby małych naczyń mózgowych (jeśli traktować tę specyficzną grupę pacjentów rozłącznie), a także OUNM z relatywnie niewielkim deficytem neurologicznym (ang. nondisabling neurologic deficit; UNM nie skutkujący istotną niepełnosprawnością), gdzie brakuje wystarczających dowodów naukowych, które skutkowałyby najwyższym poziomem rekomendacji[Karaszewski et al. 2021; Khatri et al. 2018].

W ostatnich latach występuje dynamiczny postęp w zakresie możliwości logistycznych i medycznych stosowania leczenia rekanalizacyjno-reperfuzyjnego i obserwuje się znaczny wzrost liczby wykonywanych procedur i odsetka tak leczonych pacjentów. Duże znaczenie w postępach w terapii OUNM odegrał rozwój i poprawa dostępności diagnostyki neuroobrazowej w tym przede wszystkim obrazowanie oparte na dyfuzji (DWI, diffusion-weighted imaging) rezonansu magnetycznego (MRI, magnetic resonance imaging) z możliwością oceny tkanki „zagrożonej" – objętej obrzękiem cytotoksycznym, a także angiografia i perfuzja tomografii komputerowej (CTA, computed tomography angiography, CTP, computed tomography perfusion) pozwalające na ocenę parametrów perfuzyjnych – CBV (cerebral blood volume), CBF (cerebral blood flow), MTT (mean transit time), a także stopnia rozbudowania naczyń krążenia obocznego, tzw. kolaterali[Thomalla et al. 2018; Ma et al. 2019; Nogueira et al. 2017; Albers et al. 2018].

Termin „rokowanie tkankowe” (ang. tissue outcome), czyli spodziewana ostateczna rozległość uszkodzenia tkanki z powodu ostrego, ogniskowego niedokrwienia, określa objętość uszkodzenia mózgu po jednym bądź mnogich incydentach naczyniowych w badaniu anatomostrukturalnym; in vivo można je skwantyfikować przy pomocy niektórych technik neuroobrazowych. Rokowanie tkankowe koreluje z rokowaniem klinicznym i funkcjonalnym, ale nie jest z nim tożsame.

Należy dodać, że głębokość deficytu perfuzji mózgowej jest najsilniejszym predyktorem apoptozy i nekrozy komórek nerwowych[Shimosegawa et al. 2005], ale na rokowanie tkankowe wpływa również szereg innych czynników[Tabela 1][Amantea and Bagetta 2017; Fedorovich and Waseem 2018; Wang et al. 2018a, b].

Tabela 1. Czynniki modyfikujące prawdopodobieństwo apoptozy i nekrozy komórek nerwowych w warunkach ogniskowego niedokrwienia tkanki nerwowej

Czynniki modyfikujące prawdopodobieństwo śmierci komórki
Czynniki stymulujące lub hamujące ścieżkę apoptozy
Promowanie śmierci komórki nerwowej przez kinazy aktywowane mitogenami (MAPK, mitogen-activated protein kinase)
Polimorfizmy domeny reagującej z białkiem Bcl-2 (B-cell lymphoma-2 protein) i innymi białkami proapoptotycznymi
Polimorfizmy enzymów zaangażowanych w produkcję energii w komórce
Osobnicza zmienność ekscytotoksyczności i promowanie ekscytotoksyczności neuronalnej przez kinazę białkową C (PKC, protein kinase C)
Polimorfizmy receptorowe – NMDA (rec. N-metylo-D-asparaginowy) i AMPA (rec. kwasu α-amino-3-hydroksy-5-metylo-4-izoksazolopropionowego)
Toksyczność glutaminianu
Różnorodność mechanizmów wejścia jonów Ca2+ do komórki, przeładowanie jonami Zn2+ i ich toksyczność
Zmiany stężenia dopaminy
Lokalne mechanizmy regulatorowe odpowiedzialne za produkcję reaktywnych form tlenu (ROS, reactive oxygen species)
Działanie neuroprotekcyjne niektórych neurotransmiterów – serotonina, adenozyna, kwas γ-aminomasłowy, a także czynników wzrostu (IGF-1, insulin-like growth factor), czynników neurotroficznych 4/5 (NT-4/5, neurotrophins 4/5), neurotroficznego czynnika pochodzenia mózgowego (BDNF, brain-derived neurotrophic factor), czynnika wzrostu nerwów (NGF, nerve growth factor), podstawowego czynnika wzrostu fibroblastów (bFGF, basic fibroblast growth factor)
Reakcja na post-niedokrwienną falę reperfuzyjną
Kaskada zapalenia

Wyrazem tej tezy jest na przykład istnienie tzw. odwróconego niedopasowania (reverse mismatch). W większości przypadków ostateczne uszkodzenie tkankowe, czyli obszar martwicy mózgu wtórny do niedokrwienia jest mniejszy niż obszar hipoperfuzji. Jednak w niektórych przypadkach obszar ten wykracza znacznie poza anatomiczną strefę objętą hipoperfuzją/niedokrwieniem. Pojęcie „odwróconego” mismatchu [Karaszewski et al. 2019] - DWI-T2W/FLAIR (fluid-attenuated inversion recovery), perfuzja-DWI, DWI-DWI (badanie kontrolne) - jako element wyjaśniania zjawiska odmiennego rokowania tkankowego przy „podobnych” klasycznych parametrach wyjściowych – np. podobnym obszarze tkanki z podobnym ilościowo deficytem perfuzji, podobnym stanie kolaterali, podobną wydolnością

układu sercowo-naczyniowego i autonomicznego układu nerwowego, przy braku znanych czynników klinicznych modyfikujących przebieg choroby (np. infekcje, inne) – wprowadzone zostało do literatury w pierwszej pracy stanowiącej doktorski cykl publikacji[Karaszewski et al. 2019; Stevens et al. 2014; Jiang et al. 2015; Karaszewski et al. 2010].

Należy jednak dodać, że w OUNM na rokowanie tkankowe, czyli ostateczną wielkość uszkodzenia mózgu, wpływają nie tylko mechanizmy bezpośrednio związane z niedokrwieniem tkanki, ale również uszkodzenie spowodowane wtórnym ukrwotocznieniem, które może wystąpić w naturalnym przebiegu choroby, ale może też być efektem niepożądanym stosowanego leczenia.

Dotychczasowa wiedza na temat czynników ryzyka wtórnego ukrwotocznienia po leczeniu specyficznym UNM, pozostaje dalece niewystarczająca. Dane uzyskane z rejestru SITS-MOST (The Safe Implementation of Thrombolysis in Stroke-Monitoring Study)[Wahlgren et al. 2007], identyfikują tzw. podstawowe czynniki ryzyka wtórnego ukrwotocznienia ogniska niedokrwiennego. Są to: wyjściowa ciężkość deficytu neurologicznego według NIHSS (National Institutes of Health Stroke Scale), stężenie glukozy, skurczowe ciśnienie tętnicze krwi, wywiad nadciśnienia tętniczego, wiek, masa ciała, czas od zachorowania do rozpoczęcia leczenia IVT, terapia lekiem przeciwpłytkowym, podwójna terapia przeciwpłytkowa.

Niestety, pomimo wiedzy o powyższych czynnikach ryzyka, a także pomimo uwzględniającej je odpowiedniej kwalifikacji do leczenia duża część chorych leczonych IVT rozwija powikłania krwotoczne, u 3-7% pacjentów leczonych IVT dochodzi do pogarszającego rokowanie objawowego krwawienia śródmózgowego (sICH, symptomatic intracerebral hemorrhage), zaś u jeszcze większego odsetka chorych (nawet do 27.5%[Strbian et al. 2011]) może wystąpić krwawienie anatomicznie odległe (rICH, remote-intracerebral hemorrhage), czyli zlokalizowane poza obszarem ostrego niedokrwienia, przy czym niekoniecznie musi ono skutkować jawnym pogorszeniem stanu neurologicznego.

sICH, jako najgroźniejsze powikłanie leczenia IVT, możemy zdefiniować zgodnie z kryteriami rejestru SITS-MOST jako transformację krwotoczną typu PH2 według klasyfikacji ECASS-II (parenchymal hematoma type 2, krwiak śródmiąższowy typu 2; ECASS, The European Cooperative Acute Stroke Study scale) [Hacke et al. 1995][Tabela 2], stwierdzoną w ciągu 22-36 godz. od rozpoczęcia leczenia IVT, przebiegającą z klinicznie istotnym pogorszeniem stanu neurologicznego, rozumianym przez wzrost punktacji w skali NIHSS o co najmniej 4 pkt. Wśród pacjentów rejestru SITS-MOST, leczonych IVT, odnotowano nie tylko istotnie wyższe ryzyko wystąpienia krwawienia typu PH2 (3.7% vs 0.6%, RR 6.67 (4.11-10.84)), ale również ryzyko krwawienia zakończonego zgonem (2.7% vs 0.4%, RR 7.14 (3.98-12.79)).

Tabela 2. Klasyfikacja ECASS-II (The European Cooperative Acute Stroke Study scale) – transformacja krwotoczna po leczeniu trombolitycznym dożylnym [Hacke et al. 1995]

Klasyfikacja krwawienia	Obraz radiologiczny
Zawał krwotoczny typu 1 (HI1, Hemorrhagic infarction type 1)	Niewielkie wybroczyny w obszarze zawału tkanki

Zawał krwotoczny typu 2 (HI2, Hemorrhagic infarction type 2)	Wybroczyny zlewające się w obszarze zawału tkanki; bez efektu masy
Krwiak śródmiąższowy typu 1 (PH1, Parenchymal hematoma type 1)	Homogenny obszar hiperdensyjny obejmujący <30% strefy zawału tkanki; niewielki efekt masy.
Krwiak śródmiąższowy typu 2 (PH2, Parenchymal hematoma type 2)	Homogenny obszar hiperdensyjny obejmujący >30% strefy zawału tkanki; istotny efekt masy; Każdy homogeny obszar hiperdensyjny zlokalizowany poza strefą zawału tkanki

Co więcej, wiadomo że leczenie trombolityczne jest związane nie tylko z występowaniem wtórnych krwotoków objawowych i bezobjawowych, zlokalizowanych w obszarze ogniska zawałowego, a także odległych, ale również z powstawaniem mikrokrwawień mózgowych (CMBs, cerebral microbleeds). CMBs to niewielkie, średnicy do 5 mm, okrągłe zmiany widoczne w sekwencji T2*, czy sekwencji podatności magnetycznej (SWI, susceptibility weighted imaging), jako ubytek sygnału w obrębie miąższu mózgu. Charakterystykę neuroobrazową CMBs przedstawiono w Tabeli 3.

Tabela 3. Mikrokrwawienia mózgowe – charakterystyka neuroobrazowa[Charidimou et al. 2011; Greenberg et al. 2009; Wardlaw et al. 2013]

Niewielki, okrągły ubytek sygnału otoczony przez tkankę nerwową
Lokalizacja poza obszarem zawału tkanki nerwowej
Średnica do 5 mm
Możliwość uwidocznienia w sekwencji T2* i SWI
Tzw. „blooming" effect – efekt kwitnienia w sekwencji T2*
Zazwyczaj niewidoczne w tomografii komputerowej, sekwencji FLAIR, czy T1 MRI

CMBs występują istotnie częściej w populacji ludzi starszych, zwłaszcza ze współistniejącymi czynnikami ryzyka sercowo-naczyniowego, w tym nadciśnieniem tętniczym. Warto podkreślić, że CMBs jako takie, nie wywołują „nowych" objawów klinicznych w momencie zachorowania na udar mózgu, jednakże ich całkowita liczba niesie ze sobą istotne implikacje dla przyszłych losów pacjenta, zwłaszcza w kontekście zaburzeń funkcji poznawczych[Lee et al. 2018; Poels et al. 2010; Yatawara et al. 2020].

CMBs są uważane za wskaźnik zwiększonej wrażliwości drobnych naczyń mózgowych na „czynniki uszkadzające" takie jak nadciśnienie tętnicze, czy leczenie przeciwkrzepliwe. Uważa się, że wskaźnik nasilenia CMBs w badaniu neuroobrazowym (MRI) może być kluczowym elementem oceny ryzyka wtórnego ukrwotocznienia u pacjentów nie tylko leczonych IVT, ale też kwalifikowanych do terapii doustnymi lekami przeciwkrzepliwymi (OACs, oral anticoagulants)[Wilson et al. 2019; Best et al. 2021]. W tym kontekście wskaźnik nasilenia CMBs znacząco zwiększa wartość predykcyjną modelu w opozycji do narzędzi opartych o dane wyłącznie kliniczne, jak HAS-BLED[Pisters et al. 2010].

Samo powstawanie nowych CMBs po leczeniu IVT z rtPA jest opisywane w literaturze[Jeon et al. 2009; Kimura et al. 2013; Yan et al. 2014; Braemswig et al. 2019; Miwa et al 2021; Capuana et al. 2021], jednakże z przyczyn technicznych (konieczność wykonania neuroobrazowania MRI przed podażą rtPA i badanie kontrolne) ocena prospektywna jest

niezwykle trudna, gdyż dodatkowo występuje tutaj oczywisty konflikt pomiędzy potrzebą optymalizacji czasowej podaży IVT, a „stratą" czasową na wykonanie MRI w fazie nadostrej UNM.

Należy podkreślić, że dotychczas wykorzystywane systemy stratyfikujące ryzyko transformacji krwotocznej po leczeniu IVT wykazują jedynie umiarkowaną wartość predykcyjną[Karaszewski et al. 2015] i są dalece niewystarczające w praktyce klinicznej, gdyż wciąż 3-7% pacjentów leczonych doświadcza powikłań w postaci sICH.

Istnieje zatem potrzeba opracowania modelu, który pozwalałby na precyzyjniejszą predykcję rokowania tkankowego w kontekście wtórnego ukrwotocznienia, to jest ryzyka ukrwotocznienia, szczególnie wtórnego do leczenia trombolitycznego, w tym identyfikacji i włączenia do dotychczasowych modeli nowych parametrów, które poprawią ich efektywność.

Celem niniejszej rozprawy na stopień doktora nauk medycznych było sprawdzenie hipotez, że:

- u pacjentów z OUNM obecność mikrokrwawień mózgowych zwiększa ryzyko śródczaszkowych powikłań krwotocznych w przypadku zastosowania leczenia trombolitycznego i może być dodatkowym czynnikiem w szacowaniu ryzyka tych powikłań
- u pacjentów z OUNM zwiększone bądź zmniejszone stężenie niektórych białek krwi obwodowej przed leczeniem trombolitycznym zwiększa ryzyko śródczaszkowych powikłań krwotocznych takiej terapii.

INTRODUCTION

Acute stroke is a leading cause of disability and second cause of death worldwide. According to World Health Organization (WHO) in 2019, there were 12.2 million incident cases of stroke, 6.55 million deaths from stroke (acute ischemic stroke, AIS, constituted for 2.7 million of all deaths) and 143 million years lost due to ill-health, disability or early death (DALYs)[GBD 2019 Stroke Collaborators]. Almost 85 percent of all strokes are ischemic (acute ischemic stroke, AIS). As stated in Polish National Health Fund report[NFZ o zdrowiu. Udar niedokrwienny mózgu. 2019], each year there are 70 thousands incident cases of stroke. From 2013 to 2018 the absolute number of stroke patients slightly decreased by 7.6% from 75.7 thousands to 70.7 thousands per year.

Recanalization-reperfusion therapies for AIS, combined with other management steps, have greatly improved functional outcome of victims of the disorder. Thrombolytic treatment (IVT, intravenous thrombolysis) with recombinant tissue plasminogen activator (rtPA) – more often alteplase than tenecteplase (AHA/ASA, American Heart Association/American Stroke Association and ESO, European Stroke Organisation indicate Tenecteplase's benefit in AIS with large vessel occlusion, LVO) and mechanical thrombectomy are mainstay of specific therapies for AIS. On the principles of evidence-based medicine (EBM), these therapies are supported by level A quality of scientific evidence and the highest class of recommendation in guidelines [Emberson et al. 2014; Goyal et al. 2016]. The exception from those, without any high-quality scientific evidence, is AIS due to small vessel disease and AIS with minimal, non-disabling neurologic deficit[Karaszewski et al. 2021; Khatri et al. 2018].

Recent years, we observe dynamic progress in medical and logistic possibilities of applying recanalization-reperfusion therapies with significant increase in numbers of performed procedures in stroke victims, mainly because of better access to advanced neuroimaging techniques. Magnetic resonance imaging (MRI) with diffusion-weighted imaging (DWI) for the assessment of tissue "at risk" with cytotoxic edema, together with computed tomography angiography and perfusion (CTA, CTP) for the perfusion-parameters (CBV, cerebral blood volume; CBF, cerebral blood flow; MTT, mean transit time) and collateral assessment, allowed for more personalized, exteneded management protocols in therapy of AIS[Thomalla et al. 2018; Ma et al. 2019; Nogueira et al. 2017; Albers et al. 2018].

Term "tissue outcome" is related to the expected final lesion volume following single or multiple incidents of focal cerebral ischemia; in vivo, tissue outcome could be assess and quantify using advanced neuroimaging techniques. Tissue outcome correlates with clinical and functional outcome but is not exactly the same.

Additionally, the level of tissue perfusion deficit in AIS, is the strongest predictor of neuronal apoptosis and necrosis[Shimosegawa et al. 2005], but there are other multiple factors that might modify the tissue outcome[Table 1][Amantea and Bagetta 2017; Fedorovich and Waseem 2018; Wang et al. 2018a, b].

Table 1. Factors that might modify the probability of neuronal apoptosis and necrosis following focal cerebral ischemia

Factors that might modify the probability of neuronal death
multiple factors stimulating or inhibiting apoptotic pathways

enhancement of ischemic neuronal death by mitogen-activated protein (MAP) kinases involved
polymorphisms of Bcl-2 interacting domain (BID) and other proapoptoticproteins
polymorphisms of genes of enzymes involved in energy metabolism processes
individual variability in excitotoxicity; enhancement of neuronal excitotoxicity by protein kinase C (PKC)
polymorphisms of protein peptide components of selected receptors like NMDA or AMPA
toxicity of glutamate
variability in mechanisms of Ca2+ cell entry; Zn2+ overload and toxicity
changes in dopamine concentration
local regulatory mechanisms of reactive oxygen species (ROS) production and release
neuroprotection of several neurotransmitters such as serotonin, adenosine and γ-aminobutyric acid; reduction of brain damage by growth factors including IGF-1, neurotrophins 4/5 (NT-4/5), brain-derived neurotrophic factor (BDNF), nerve growth factor (NGF), basic fibroblast growth factor reactions after postischemic reperfusion inflammatory cascade
reactions after postischemic reperfusion
inflammatory cascade

The existence of phenomenon called “reverse mismatch” supports that thesis. In most cases final extent of the brain damage following AIS is smaller than initial perfusion deficit. However, in the minority of cases, that final lesion volume expands much beyond the anatomical area of perfusion deficit/ischemia. “Reverse mismatch” phenomenon[Karaszewski et al. 2019] – a reverse DWI-T2W/FLAIR (fluid-attenuated inversion recovery), a reverse perfusion – DWI, or a reverse DWI-DWI (follow-up) – might be responsible for different tissue outcome in patients exposed to similarly characterized focal brain ischemia – similar initial perfusion deficit, similar collaterals, similar cardiovascular and autonomic nervous system sufficiency, with no confounders like infections. Term “reverse mismatch” was introduced to literature in the first publication of this doctoral thesis[Karaszewski et al. 2019; Stevens et al. 2014; Jiang et al 2015; Karaszewski et al. 2010].

It is worth noting that the final extent of the brain damage following AIS, depends not only on multiple factors directly related to ischemia, but also related to secondary hemorrhage. Secondary hemorrhage could be a complication of administered treatment or be a phenomenon associated with natural course of the disease.

Until now, the knowledge about risk factors for rtPA-associated secondary hemorrhage is still insufficient. The SITS-MOST registry (The Safe Implementation of Thrombolysis in Stroke-Monitoring Study)[Wahlgren et al. 2007] identified basic risk factors for secondary hemorrhage: baseline NIHSS (National Institutes of Health Stroke Scale) score, serum glucose, systolic blood pressure, history of hypertension, age, body weight, stroke onset to treatment time, antiplatelet monotherapy, and dual antiplatelet therapy.

Unfortunately, despite of knowledge about above mentioned risk factors, and after detailed assessment of the inclusion/exclusion criteria to IVT, the substantial portion of cases will be complicated by post-rtPA secondary hemorrhage – symptomatic intracerebral hemorrhage (sICH) occurs in 3-7 percent of cases and remote intracerebral hemorrhage (rICH), located remotely from the lesion, mostly without any obvious clinical deterioration, in up to 27.5 percent of incidents[Strbian et al. 2011].

sICH, known as the most dangerous IVT-associated complication, could be defined according to SITS-MOST registry criteria – PH2 type hemorrhagic transformation in ECASS-II classification (parenchymal hematoma type 2; The European Cooperative Acute Stroke Study scale)[Hacke et al. 1995][Table 2] within 22–36h after IVT administration with the clinically important deterioration of neurological status, defined as deterioration of 4 or more points on the NIHSS score. SITS-MOST registry revealed not only higher frequency of PH2 [3.7% vs 0.6%, OR 6.67 (4.11-10.84)] but also fatal intracerebral hemorrhage [2.7% vs 0.4%, OR 7.14 (3.98-12.79)] in IVT group.

Table 2. The European Cooperative Acute Stroke Study scale of the hemorrhagic transformation after the thrombolytic treatment [Hacke et al. 1995]

Hemorrhage classification	Radiographic appearance
Hemorrhagic infarction type 1 (HI1)	Small hyperdense petechiae.
Hemorrhagic infarction type 2 (HI2)	More confluent hyperdensity throughout the infarct zone; without mass effect.
Parenchymal hematoma type 1 (PH1)	Homogeneous hyperdensity occupying <30% of the infarct zone; some mass effect.
Parenchymal hematoma type 2 (PH2)	Homogeneous hyperdensity occupying >30% of the infarct zone; significant mass effect. Or, any homogenous hyperdensity located beyond the borders of the infarct zone.

Moreover, IVT might also result in another type of hemorrhagic complication – the cerebral microbleeds (CMBs). CMBs are small, rounded lesions surrounded by brain tissue with diameter up to 5 mm, detected on T2* or SWI (susceptibility-weighted imaging) as a signal loss. The CMBs neuroimaging characteristics are listed in Table 3.

Table 3. Cerebral microbleeds – neuroimaging characteristics [Charidimou et al. 2011; Greenberg et al. 2009; Wardlaw et al. 2013]

Small, rounded signal loss lesions surrounded by brain tissue
Located outside the infarcted area
Diameter up to 5 mm
Detected on T2*-weighted and SWI
Blooming effect on T2*-weighted MRI
Generally not seen on computed tomography, FLAIR, T1-weighted MRI

The prevalence of CMBs is significantly higher in elderly population, especially with coexisting cardiovascular risk factors as hypertension. It is worth noting that CMBs usually remain clinically silent in terms of AIS, but might have cumulative impact on patients in the following years, mainly because of their connection with cognitive decline[Lee et al. 2018; Poels et al. 2010; Yatawara et al. 2020].

We believe, that CMBs burden in MRI study might be crucial for the assessment of the risk of secondary hemorrhage due to IVT treatment or due to oral anticoagulant therapy

(OACs)[Wilson et al. 2019; Best et al. 2021]. Moreover, CMBs burden alone or combined with other selected characteristics may be more predictive of sICH than tools based solely on clinical parameters, including HAS-BLED.

The association between formation of new CMBs and IVT is extensively discussed in literature[Jeon et al. 2009; Kimura et al. 2013; Yan et al. 2014; Braemswig et al. 2019; Miwa et al 2021; Capuana et al. 2021], albeit the prospective assessment is difficult. Technically, the need for double MRI-testing (before IVT and follow-up), as well as obvious conflict of interest between the optimal timing of IVT and MRI testing before rtPA administration, are major limitations in this and other studies.

It should be emphasized that previously used tools and scoring systems for the risk of IVT-related secondary hemorrhage perform poorly and have only modest predictive value for identifying patients at risk[Karaszewski et al. 2015]. The result is that still 3-7 percent of patients develop sICH.

There is a need to develop new tool/scoring system with better predictive value for prospective assessment of tissue outcome in terms of the risk of secondary hemorrhage, mainly related to IVT, by identification and applying new neuroimaging and biochemical parameters.

Aims of this doctoral thesis:

- it is hypothesized that in patients with AIS, the presence of baseline CMBs increase the risk of IVT-related secondary hemorrhage, and that baseline CMBs might be a new neuroimaging parameter for prospective assessment of that risk;
- it is hypothesized that in patients with AIS any change in peptide/protein concentration before rtPA administration might potentially increase the risk of IVT-related secondary hemorrhage.

OMÓWIENIE PUBLIKACJI WCHODZĄCYCH W SKŁAD ROZPRAWY DOKTORSKIEJ

Pracę doktorską zaplanowano jako cykl trzech artykułów naukowych opublikowanych w czasopismach posiadających IF – jednej poglądowej i dwóch oryginalnych (które stanowią zasadnicze komponenty cyklu).

Publikacja 1, praca poglądowa – Karaszewski, B., Jabłoński, B., Żukowicz, W. The salvageable brain in acute ischemic stroke. The concept of a reverse mismatch: a mini-review. Metab Brain Dis. 2020 Feb;35(2):237-240.
Punktacja IF: 3.584.
Punktacja MEiN: 70.000.

W pracy wyeksponowano mnogość czynników wpływających na rokowanie tkankowe po udarze niedokrwiennym mózgu, także konstytutywnych - niewiązanych z bieżącym incydentem mózgowo-naczyniowym, innych niż tylko wielkość obszaru i stopnień upośledzenia perfuzji tkankowej.

Artykuł wprowadza pojęcie „odwróconego mismatchu" (reverse mismatch) – niedopasowania pomiędzy m.in. sekwencjami DWI i T2W/FLAIR, perfuzyjnymi i DWI, DWI wyjściowym i DWI kontrolnym, który jest manifestacją nierzadko obserwowanego w klinice zjawiska - odmiennego rokowania tkankowego pomimo „podobnych" podstawowych parametrach wyjściowych – podobnej rozległości obszaru tkanki z deficytem perfuzji, podobnego stanu funkcjonalnego kolaterali, wydolności układu sercowo-naczyniowego i autonomicznego układu nerwowego i innych oraz przy nieobecności powikłań, które występują w ciągu pierwszych dób po udarze i wpływają na rokowanie tkankowe (np. infekcje, kardiomiopatia takotsubo). W praktyce oznacza to, że w niektórych przypadkach obszar martwicy mózgu wtórny do ogniskowego niedokrwienia jest większy niż wyjściowy obszar krytycznego obniżenia perfuzji mózgowej, co niejako potwierdza, że na rokowanie tkankowe wpływają, oprócz samej hipoperfuzji, również inne czynniki – biochemiczne, genetyczne.

Ponadto, w artykule podsumowano najważniejsze osiągniecia ostatnich lat w zakresie rozszerzania możliwości zastosowań leczenia rekanalizacyjno-reperfuzyjnego poza tzw. klasycznymi kryteriami kwalifikacji, najczęściej z zastosowaniem bardziej zaawansowanych metod diagnostyki neuroobrazowej - rezonansu magnetycznego z oceną rozległości obrzęku cytotoksycznego w sekwencji DWI, a także angiografii i perfuzji tomografii komputerowej z oceną parametrów perfuzyjnych – CBV, CBF, MTT oraz stopnia rozbudowania naczyń krążenia obocznego, tzw. kolaterali.

Publikacja 2, praca <u>oryginalna</u> – Jabłoński, B., Gójska-Grymajło, A., Ossowska, D., Szurowska, E., Wyszomirski, A., Rojek, B., Karaszewski, B. New remote cerebral microbleeds on T2*-Weighted Echo Planar Magnetic Resonance Imaging after intravenous thrombolysis for acute ischemic stroke. Front Neurol. 2022; 12:744701.
Published 2022 Feb 15.
Punktacja IF: 4.003.
Punktacja MEiN: 100.000.

Cele
Badanie prospektywne z oceną całkowitej liczby CMBs przed i po leczeniu IVT, a także określeniem korelacji pomiędzy występowaniem CMBs a ryzykiem transformacji krwotocznej.

Ograniczone dane empiryczne wskazują, że leczenie IVT jest związane nie tylko z występowaniem wtórnych krwotoków objawowych i bezobjawowych zlokalizowanych tak w obszarze ogniska niedokrwiennego (najczęściej), jak i odległych od niego, ale również z powstawaniem CMBs. CMBs to niewielkie, średnicy do 5 mm, okrągłe zmiany widoczne w sekwencji T2*, czy SWI, jako ubytek sygnału w obrębie miąższu mózgu. Występują istotnie częściej w populacji ludzi starszych, zwłaszcza ze współistniejącymi czynnikami ryzyka sercowo-naczyniowego, a szczególny związek upatruje się tu z wieloletnim nadciśnieniem tętniczym. Warto podkreślić, że CMBs jako takie, nie wywołują „nowych" objawów klinicznych w momencie zachorowania na udar mózgu nawet jeśli wystąpią z nim jednoczasowo, jednakże ich całkowita liczba z uwzględnieniem lokalizacji (burden) niesie ze sobą istotne implikacje dla przyszłych losów pacjenta, zwłaszcza w kontekście rozwoju zaburzeń funkcji poznawczych.
CMBs są ponadto uważane za wskaźnik zwiększonej wrażliwości drobnych naczyń mózgowych na czynniki uszkadzające, takiej jak nadciśnienie tętnicze, czy leczenie przeciwkrzepliwe. Podjęto próby zaimplementowania wskaźnika nasilenia CMBs w badaniu neuroobrazowym (MRI) do modelu stratyfikacji ryzyka sICH u pacjentów leczonych trombolitycznie, czy kwalifikowanych do terapii lekami przeciwkrzepliwymi (OACs, oral anticoagulants). W tym kontekście wskaźnik nasilenia CMBs znacząco zwiększa wartość predykcyjną modelu w opozycji do narzędzi opartych o dane kliniczne, jak HAS-BLED.
Samo powstawanie nowych CMBs po leczeniu IVT z rtPA jest opisywane w literaturze, jednakże z przyczyn technicznych (konieczność wykonania neuroobrazowania MRI przed podażą rtPA i badanie kontrolne) ocena prospektywna jest trudna.
W naszym badaniu podjęliśmy zadania weryfikacji trzech hipotez:

- że leczenie IVT zwiększa ryzyko powstawania nowych CMBs
- że wyjściowe występowanie CMBs jest istotnym czynnikiem ryzyka powstawania nowych CMBs
- że wyjściowe występowanie CMBs jest istotnym czynnikiem ryzyka transformacji krwotocznej.

Materiał i metody

- **Pacjenci:** 49 chorych Kliniki Neurologii Dorosłych Gdańskiego Uniwersytetu Medycznego / Uniwersyteckiego Centrum Klinicznego w Gdańsku z rozpoznaniem UNM, zakwalifikowanych do leczenia IVT pomiędzy 20.03.2019 a 19.10.2020.
- **Ocena kliniczna:** ocena kliniczna doświadczonego neurologa specjalizującego się w udarze mózgu; etiologizacja UNM zgodnie z klasyfikacją TOAST (Trial of Org 10172 in Acute Stroke Treatment) – choroba dużych naczyń (LVD, large-vessel disease), udar sercowo-zatorowy (CE, cardioembolic stroke), choroba małych naczyń (SVD, small vessel disease), udar mózgu o nieustalonej etiologii (UE, stroke of unknown etiology) i udar mózgu o rzadkiej etiologii (stroke of rare etiology).
- **Ocena neuroobrazowa:** wszystkie badania MRI mózgowia zostały wykonane aparatem 1.5T Siemens Magnetom Aera system:
a. badanie wyjściowe MRI, przed leczeniem IVT, według protokołu GoBrain (sekwencje: T1 GRE (gradient recalled echo, sekwencja echa gradientowego), TSE (turbo-spin echo, sekwencja echa spinowego), FLAIR, DWI, T2*-EPI (echo-planar imaging, sekwencja echa planarnego) – protokół skrócony, dedykowany pacjentom w ostrej fazie UNM [Rapalino et al. 2016]; czas akwizycji obrazów – 5.5 min.
b. kontrolne badanie TK bez kontrastu (ncCT, non-contrast computed tomography) 22-36 godz. od rozpoczęcia leczenia IVT.
c. badanie kontrolne MRI w 7-9 dobie hospitalizacji – według „pełnego protokołu" (sekwencje: T1 GRE, TSE, FLAIR, DWI, T2*-EPI, DTI (diffusion tensor imaging, obrazowanie tensora dyfuzji), SWI.
d. Detekcja CMBs – T2*-weighted EPI-GRE; ocena manualna przez trzech badaczy – neurologa (BJ) oraz radiologa współpracującego z fizykiem (ESz, DO).
W przypadkach, w których zaistniała taka potrzeba, do oceny CMBs wykorzystano, oprócz sekwencji T2*-weighted EPI-GRE, również sekwencję SWI.
e. ocena transformacji krwotocznej według klasyfikacji ECASS-II; definicja sICH według rejestru SITS-MOST.
Do oceny objętości wyjściowego ogniska niedokrwiennego wykorzystano sekwencję DWI, zaś do oceny nasilenia zmian istoty białej według klasyfikacji Fazekasa[Fazekas et al. 1987] – sekwencję Axial T2 FLAIR.
- **Analiza statystyczna:** wszystkie analizy statystyczne przeprowadzone zostały w pakiecie statystycznym R (wersja 3.6.3). Podstawowe charakterystyki grupy badawczej podsumowano jako średnie z odchyleniami standardowymi (SD, standard deviation), mediany z dolnymi i górnymi kwartylami, liczności z wartościami procentowymi. Różnice w rozkładach zmiennych typu ciągłego pomiędzy dwiema niezależnymi grupami pacjentów zweryfikowano testem t Studenta lub testem U Manna-Whitneya. Test chi kwadrat lub dokładny test Fishera zastosowano do weryfikacji różnic zmiennych kategorycznych pomiędzy dwiema niezależnymi grupami pacjentów. Wyniki wieloczynnikowej regresji przedstawiono jako ryzyko względne (RR, risk ratio) z 95% przedziałem ufności (CI, confidence interval). Hipotezy badawcze weryfikowano testami dwustronnymi, a wartości p poniżej 0.05 uznano za istotne statystycznie.

Wyniki

W badaniu MRI GoBrain (sekwencja T2*-EPI-GRE), przed leczeniem IVT z podażą rtPA, uwidoczniono sumarycznie 37 CMBs u 14 (28.6%) pacjentów; u jednego pacjenta liczba CMBs wynosiła > 3. W ocenie kontrolnej MRI (T2*-EPI-GRE, w razie potrzeby weryfikacja SWI) całkowita liczba CMBs wyniosła 103; nowe CMBs odnotowano u 5 (14.3%) spośród 35 pacjentów, u których wyjściowo nie stwierdzono żadnych CMBs i u 9 (64.3%) spośród 14 chorych z wyjściowo stwierdzanymi CMBs. Pacjenci, u których stwierdzono powstanie nowych CMBs byli starsi (p=0.026), mieli wyższe stężenie kreatyniny (p=0.035) i częściej prezentowali CMBs w badaniu wyjściowym (p<0.001), podczas gdy na pojawienie się nowych CMBs wpływu nie miały współwystępowanie nadciśnienia tętniczego, ciężkość deficytu neurologicznego wyrażona w skali NIHSS, podtyp UNM według klasyfikacji TOAST, stopień nasilenia zmian istoty białej według klasyfikacji Fazekasa, a także objętość wyjściowego ogniska niedokrwiennego w sekwencji DWI.
U 10 (20.4%) pacjentów wystąpiła transformacja krwotoczna - według klasyfikacji ECASS: 6 HI1, 2 HI2, 1 PH1, 1 PH2.
W analizie wieloczynnikowej wykazano, że obecność CMBs w badaniu wyjściowym (Risk Ratio 5.95, 95% przedział ufności 2.69-13.20, p<0.001) i niższy poziom płytek krwi (Risk Ratio 0.992, 95% przedział ufności 0.986-0.998, p=0.007) korelowały w sposób istotny z powstaniem nowych CMBs po leczeniu IVT.

Ocena jakości kwantyfikacji CMBs została przedstawiona w Tabeli 5 – uzyskane wartości współczynnika kappa Cohena świadczą o istotnej zgodności pomiędzy obserwatorami.

Tabela 4. Zgodność między obserwatorami w ocenie MRI mikrokrwawień mózgowych (CMBs)

CMBs lokalizacja w MRI	Badanie wyjściowe [kappa]*	Ocena kontrolna [kappa]*
Struktury głębokie	0.64	0.78
Struktury korowe/podkorowe	0.58	0.74
Wszystkie	0.63	0.77

* zgodność między obserwatorami została zbadana wykorzystując współczynnik kappa Cohena; dla poszczególnych wartości: 0.01-0.20 niska zgodność, 0.21-0.40 dostateczna zgodność, 0.41-0.60 umiarkowana zgodność, 0.61-0.80 istotna zgodność, >0.80 niemal idealna zgodność.

Wniosek

Wykazaliśmy, że obecność CMBs w badaniu wyjściowym (Risk Ratio 5.95, 95% przedział ufności 2.69-13.20, p<0.001) zwiększała ryzyko powstawania nowych CMBs, a zatem pogarszała wskaźnik CMBs. Kolejne prace powinny zaadresować ten problem z uwzględnieniem odległego znaczenia rokowniczego – funkcjonalnego, to jest sprawdzić czy istnieje związek pomiędzy wskaźnikiem CMBs przed-po leczeniu IVT OUNM i rozwojem zaburzeń poznawczych. W badaniu nie stwierdziliśmy korelacji pomiędzy występowaniem CMBs w badaniu wyjściowym, a ryzykiem transformacji krwotocznej, co stoi w opozycji do danych literaturowych [Charidimou et al. 2015; Zand et al. 2017; Capuana et al. 2021; Charidimou et al. 2017]. Pośród potencjalnych przyczyn tych rozbieżności należy rozważyć niewielką liczbę CMBs stwierdzonych wyjściowo w badanej kohorcie - tylko u jednego pacjenta > 3 CMBs, podczas gdy wartością najczęściej podawaną w literaturze w tym

kontekście [Zand et al. 2017] jest > 10 CMBs oraz to, że do badaniu z definicji nie włączano pacjentów z zamknięciem dużego naczynia – zakwalifikowanych do leczenia mechanicznego, a zatem tych z największymi ogniskami niedokrwiennymi w neuroobrazowaniu i największymi deficytami neurologicznymi. Wyzwaniem była precyzyjna kwantyfikacja CMBs w oparciu o sekwencję T2*EPI-GRE – krótszą czasowo, ale mniej czułą dla detekcji tej patologii niż sekwencja SWI. Dlatego, w przypadkach wątpliwych lub niejednoznacznych, dla potwierdzenia lub wykluczenia obecności CMBs wykorzystano sekwencję SWI. Również z przyczyn technicznych - do analizy wskaźnika CMBs nie włączaliśmy CMBs zlokalizowanych w obszarze ogniskowego niedokrwienia mózgu, niezależnie od występowania transformacji krwotocznej i ciężkości tejże.

Należy podkreślić, że stopień zgodności oceny CMBs pomiędzy obserwatorami, wyrażony współczynnikiem kappa Cohena, określono na poziomie 0.63 (badanie wyjściowe) i 0.77 (badanie kontrolne), co świadczy o istotnym poziomie zgodności. Aby zwiększyć powtarzalność kolejnych badań i zminimalizować wpływ ułożenia pacjenta/ustawienia głowy w trakcie badania, wykorzystano opcję AutoAlign z funkcją automatycznego pozycjonowania warstwy. Dzięki tej modalności MRI, a także w związku z grubością pojedynczej warstwy – ryzyko dublowania CMBs w trakcie oceny manualnej zostało znacząco zminimalizowane.

Inne istotne ograniczenia metody to niewielka grupa badana, brak grupy kontrolnej pacjentów nie-trombolizowanych (CMBs mogą pojawiać się de novo we wczesnej fazie OUNM także u pacjentów, którzy nie otrzymali IVT choć z mniejszym prawdopodobieństwem[Charidimou et al. 2013]) oraz wykorzystanie aparatu MRI o stosunkowo niskiej polowości (1.5 T).

W kontekście liczebności grupy badanej, mamy nadzieję na zwiększenie całkowitej liczby zakwalifikowanych pacjentów w miarę kontynuowania projektu (w niniejszej publikacji zaprezentowano wyniki uzyskane w ramach fazy pilotażowej projektu własnego realizowanego w oparciu o finansowanie – grant od SIEMENS Healthineers, główny badacz prof. dr hab. n. med. Bartosz Karaszewski).

Wydaje się, że obecność nowych CMBs wespół z innymi, określonymi czynnikami klinicznymi, może znaleźć zastosowanie w predykowaniu odległego rokowania po leczeniu trombolitycznym udaru niedokrwiennego mózgu.

Publikacja 3, praca <u>oryginalna</u> – Karaszewski, B., Gójska-Grymajło, A., Czaplewska, P., Jabłoński, B., Lewandowska, A., Ossowska, D., Wyszomirski, A., Hałas, M., Szurowska, E. SWATH-MS for prospective identification of protein blood biomarkers of rtPA-associated intracranial hemorrhage in acute ischemic stroke: a pilot study. Sci Rep 11, 18765 (2021).
Finansowanie projektu – Siemens Healthineers, grant Gdańskiego Uniwersytetu Medycznego 2018, Główny Badacz – prof. dr hab. n. med. Bartosz Karaszewski.
Punktacja IF: 4.380.
Punktacja MEiN: 140.000.

Cele
Sprawdzenie hipotezy, że u pacjentów z OUNM zwiększone bądź zmniejszone stężenie niektórych białek i peptydów krwi obwodowej (złożone interakcje) przed leczeniem trombolitycznym zwiększa ryzyko śródczaszkowych powikłań krwotocznych takiej terapii (pośrednio, że addytywnie do innych czynników ryzyka ukrwotocznienia, biomarkery takie mogą istotnie wspomóc szacowanie ryzyka wystąpienia tego powikłania).

W artykule zaprezentowano ideę, metodologię opartą o nowy paradygmat badawczy (hypothesis free approach) oraz wyniki fazy pilotażowej większego projektu pozostającego w trakcie realizacji (grant realizowany przez Gdański Uniwersytet Medyczny, główny badacz - prof. dr hab. n. med. Bartosz Karaszewski). Celem projektu w całości jest opracowanie wysoce czułego i specyficznego personalizowanego narzędzia do szacowania ryzyka powikłań krwotocznych u pacjentów poddawanych leczeniu trombolitycznemu uwzgledniającego mnogie dane – kliniczne, neuroobrazowe, miRNA i proteomiczne krwi obwodowej, podczas gdy pilotażowe wyniki przedstawione w pracy będącej elementem cyklu doktorskiego zawierają tylko część ostatnią (biomarkery białkowe).

Materiał i metody
- **Pacjenci:** 41 chorych Kliniki Neurologii Dorosłych Gdańskiego Uniwersytetu Medycznego / Uniwersyteckiego Centrum Klinicznego w Gdańsku z rozpoznaniem UNM, zakwalifikowanych do leczenia IVT pomiędzy 20.03.2019 a 20.02.2020.
- **Ocena kliniczna:** ocena kliniczna doświadczonego neurologa specjalizującego się w udarze mózgu; etiologizacja UNM zgodnie z klasyfikacją TOAST (Trial of Org 10172 in Acute Stroke Treatment) – choroba dużych naczyń (LVD, large-vessel disease), udar sercowo-zatorowy (CE, cardioembolic stroke), choroba małych naczyń (SVD, small vessel disease), udar mózgu o nieustalonej etiologii (UE, stroke of unknown etiology) i udar mózgu o rzadkiej etiologii (stroke of rare etiology).
- **Ocena neuroobrazowa:** wszystkie badania MRI mózgowia zostały wykonane aparatem 1.5T Siemens Magnetom Aera system:
a. badanie wejściowe MRI, przed leczeniem IVT, według protokołu GoBrain (sekwencje: T1 GRE, TSE, FLAIR, DWI, T2*-EPI) – protokół skrócony, dedykowany pacjentom w ostrej fazie UNM [Rapalino et al. 2016]; czas akwizycji obrazów – 5.5 min.
b. kontrolne badanie ncCT 22-36 godz. od rozpoczęcia leczenia IVT.
c. badanie kontrolne MRI w 5-9 dobie hospitalizacji – według „pełnego protokołu" (sekwencje: T1 GRE, TSE, FLAIR, DWI, T2*-EPI, DTI, SWI).

d. ocena transformacji krwotocznej według klasyfikacji ECASS-II; definicja sICH według rejestru SITS-MOST.
- **Ocena biochemiczna:** materiał biologiczny (osocze, surowica) pozyskany przed leczeniem IVT; analiza proteomiczna ilościowa i półjakościowa z wykorzystaniem metodologii SWATH-MS bez znakowania izotopowego.
- **Analiza statystyczna:** wszystkie analizy statystyczne przeprowadzone zostały w pakiecie statystycznym R (wersja 3.6.3). Podstawowe charakterystyki grupy badawczej podsumowano jako średnie z odchyleniami standardowymi (SD), mediany z dolnymi i górnymi kwartylami, liczności z wartościami procentowymi. Różnice w rozkładach zmiennych typu ciągłego pomiędzy dwiema niezależnymi grupami pacjentów zweryfikowano testem t Studenta lub testem U Manna-Whitneya. Test chi kwadrat lub dokładny test Fishera zastosowano do weryfikacji różnic zmiennych kategorycznych pomiędzy dwiema niezależnymi grupami pacjentów. Wyniki wieloczynnikowej regresji przedstawiono jako ryzyko względne (RR) z 95% przedziałem ufności (CI). Hipotezy badawcze weryfikowano testami dwustronnymi, a wartości $p < 0.05$ uznano za istotne statystycznie.

Wyniki
Powtórne (follow-up) badanie ncCT w 22-36 godz. od rozpoczęcia leczenia IVT i kontrolne badanie MRI (pełen protokół) w 5-9 dobie hospitalizacji, uwidoczniły ICH u 9 pacjentów (21.95%) – ocena według klasyfikacji ECASS-II.
Na podstawie przeprowadzonych analiz próbek krwi pobranych przed leczeniem IVT, w tym wizualizacji sieci interakcji molekularnych w oprogramowaniu Cytoscape, zidentyfikowano 15 różnych białek (osiem w surowicy, siedem w osoczu)[Tabela 4], których stężenie różniło się w sposób istotny statystycznie, $p<0.05$, w zależności od tego czy doszło do badanego powikłania.

Wniosek
Analiza proteomiczna ilościowa / półjakościowa SWATH-MS (Sequential Window Acquisition of All Theoretical Mass Spectra) surowicy/osocza może przyczynić się do opracowania bardziej specyficznych/selektywnych modeli szacowania ryzyka transformacji krwotocznej po leczeniu IVT w porównaniu z modelami opartymi wyłącznie o parametry kliniczne i neuroobrazowe.
Z uwagi na niewielką grupę badaną (pilotaż dużego projektu) nie możemy jeszcze sformułować definitywnych wniosków dotyczących patofizjologii transformacji krwotocznej po leczeniu IVT w kontekście przekrojowej analizy proteomicznej surowicy/osocza. Pozyskane w fazie pilotażowej wyniki wskazują na wysokie prawdopodobieństwo pozyskania silnych biomarkerów predykcyjnych wraz z powiększeniem próbki badanej (wyznaczonej prospektywnie na podstawie odpowiednich kalkulacji statystycznych).

Tabela 5. Surowicze i osoczowe białka / peptydy “kandydaci” - biomarkery w prognozowaniu ryzyka wtórnego krwotoku śródmózgowego po leczeniu trombolizą dożylną u pacjentów z ostrym udarem niedokrwiennym mózgu

		Surowica		Osocze	
Uniprot ID	**Nazwa białka**	**p**	**Zmiana stężenia, rząd**	**p**	**Zmiana stężenia, rząd**
Q96PD5	N-acetylmuramoyl-L-alanino amidaza	**0.005**	**0.804**	0.115	1.138
P08697	Alfa-2-antyplazmina	**0.008**	**0.616**	0.614	0.935
P02768	Albumina w surowicy	**0.009**	**1.372**	0.682	1.038
P05543	Globulina wiążąca tyroksynę	**0.011**	**0.598**	0.592	1.158
P02790	Hemopeksyna	**0.015**	**0.676**	0.614	0.994
P01861	Immunoglobulin heavy constant gamma 4	**0.024**	**3.618**	0.950	1.056
P01019	Angiotensynogen	**0.037**	**0.747**	0.508	0.980
P02749	Beta-2-glikoproteina 1	**0.044**	**0.718**	0.413	1.118
P04278	Glikoproteina wiążąca hormony płciowe	0.889	1.002	**0.006**	**1.483**
P02675	Łańcuch beta fibrynogenu	0.313	0.760	**0.017**	**1.377**
P02679	Łańcuch gamma fibrynogenu	0.164	0.765	**0.021**	**1.230**
A0A0C4DH38	Immunoglobulin heavy variable-5-51	0.999	1.106	**0.021**	**1.779**
Q06033	Inter-alfa-trypsin inhibitor heavy chain H3	0.297	0.852	**0.025**	**1.213**
P02649	Apolipoproteina E	0.487	1.105	**0.027**	**1.532**
P36955	Pigment epithelium-derived factor	0.651	0.909	**0.038**	**1.270**

PODSUMOWANIE

Leczenie IVT jest obok trombektomii mechanicznej podstawową metodą terapii rekanalizacyjno-reperfuzyjnej OUNM, znacząco poprawiającą rokowanie w tej grupie pacjentów. W ostatnich latach dokonał się dynamiczny postęp w zakresie możliwości logistycznych i medycznych stosowania leczenia rekanalizacyjno-reperfuzyjnego, ze wzrastającą liczbą wykonywanych procedur i odsetkiem tak leczonych pacjentów, a także rozwojem i poprawą dostępności zaawansowanych metod neuroobrazowania, przede wszystkim obrazowania opartego na dyfuzji rezonansu magnetycznego z oceną tkanki „zagrożonej", a także angiografii i perfuzji tomografii komputerowej.

Myślą przewodnią mojej rozprawy doktorskiej jest złożona charakterystyka czynników wpływających na rokowanie pacjenta po udarze niedokrwiennym mózgu, w tym na tzw. rokowanie tkankowe.

W pracach cyklu zwrócono uwagę, że rokowanie tkankowe uzależnione jest nie tylko od parametrów związanych ze zmianami perfuzji (to jest, że pogarsza je nie tylko rozległość i głębokość deficytu perfuzji tkankowej), ale również od innych czynników – zarówno konstytutywnych, wyeksponowanych w pracy poglądowej[Karaszewski et al. 2020] oraz potencjalnie modyfikowalnych, w tym takich, które prowadzą do wtórnego ukrwotocznienia. To ostatnie wystąpić może w naturalnym przebiegu choroby, ale prawdopodobieństwo tego powikłania rośnie w przypadku podaży leczenie trombolitycznego, chociaż stwierdzenie to należy rozpatrywać w kontekście średnio jednoznacznie istotnie korzystnego wpływu rokowniczego takiej terapii.

Niemniej, pomimo prawidłowej kwalifikacji do IVT (rezygnacja u pacjentów z istotnymi zdefiniowanymi czynnikami ryzyka), część chorych rozwija powikłania krwotoczne, w tym sICH, co dotyczy 3-7% pacjentów i wiąże się z gorszym 90-dniowym rokowaniem (stan funkcjonalny) i wyższym odsetkiem niepełnosprawności niż u pacjentów nieleczonych.

Dotychczas wykorzystywane systemy stratyfikujące ryzyko transformacji krwotocznej po leczeniu IVT wykazują jedynie umiarkowaną wartość predykcyjną[Karaszewski et al. 2015] i choć częściowo użyteczne w praktyce klinicznej, wymagają doskonalenia, to jest powiększenia mocy predykcyjnej w kontekście ryzyka wtórnego ukrwotocznienia, w tym identyfikacji i włączenia do dotychczasowych modeli nowych parametrów. Takimi parametrami mogą być klinicznie zazwyczaj niejawne, obecne przed leczeniem OUNM, skutki wcześniej istniejących patologii naczyń i/lub układu krzepnięcia np. CMBs albo bieżące szeroko pojęte złożone zmiany biochemiczne krwi obwodowej wpływające na jej parametry reologiczne.

W kontynuacji tych rozważań, celem mojej pracy doktorskiej było sprawdzenie empiryczne sprawdzenie następujących hipotez:

- u pacjentów z OUNM wyjściowa obecność mikrokrwawień mózgowych zwiększa ryzyko śródczaszkowych powikłań krwotocznych w przypadku zastosowania leczenia trombolitycznego i może być dodatkowym czynnikiem w szacowaniu ryzyka tych powikłań

- u pacjentów z OUNM stężenia niektórych białek krwi obwodowej przed leczeniem trombolitycznym – pojedynczych bądź w bardziej złożonych wzorach – związane jest z ryzykiem śródczaszkowych powikłań krwotocznych wtórnych do takiej terapii

W pracy „New remote cerebral microbleeds on T2*-Weighted Echo Planar Magnetic Resonance Imaging after intravenous thrombolysis for acute ischemic stroke" wykazano, że występowanie wyjściowo CMBs jest niezależnym czynnikiem ryzyka powstawania nowych CMBs po leczeniu IVT, natomiast nie wykazano istotnej statystycznie korelacji pomiędzy wyjściowo stwierdzanymi CMBs a ryzykiem transformacji krwotocznej. Potencjalny związek pomiędzy IVT i ryzykiem występowania nowych CMBs może mieć odległe implikacje kliniczne, w tym również w kontekście ryzyka rozwoju zaburzeń funkcji poznawczych (temat powiązania CMBs z zaburzeniami funkcji poznawczych jest opisywany szeroko w literaturze, odpowiednie cytacje w bibliografii rozprawy doktorskiej), ale na tym etapie związek ten należy traktować wyłącznie jako hipotezę popartą przesłankami, która wymaga dalszych badań. Brak związku pomiędzy wyjściową obecnością CMBs i transformacją krwotoczną w badanej kohorcie – inaczej niż wykazano w niektórych innych pracach – wynika m.in. z innej struktury klinicznej badanej grupy pacjentów (NIHSS, neuroobrazowanie – z definicji nie rekrutowano pacjentów z zamknięciem dużego naczynia) oraz znacząco mniejszej wyjściowej liczby CMBs.

W pracy „SWATH-MS for prospective identification of protein blood biomarkers of rtPA-associated intracranial hemorrhage in acute ischemic stroke: a pilot study" sprawdzono hipotezę, że u pacjentów z OUNM zwiększone bądź zmniejszone stężenie niektórych białek i/lub peptydów krwi obwodowej przed leczeniem trombolitycznym zwiększa ryzyko śródczaszkowych powikłań krwotocznych takiej terapii. Z uwagi na niewielką grupę badaną (pilotaż dużego projektu) nie możemy jeszcze sformułować definitywnych wniosków dotyczących patofizjologii transformacji krwotocznej po leczeniu IVT w kontekście przekrojowej analizy proteomicznej surowicy/osocza, ale przedstawione w pracy wyniki wskazują na wysokie prawdopodobieństwo pozyskania silnych – zdefiniowanych biomarkerów predykcyjnych po powiększeniu próbki badanej (ta ostatnia została wyznaczona prospektywnie na podstawie odpowiednich kalkulacji statystycznych).

Uzyskane w cyklu prac składających się na rozprawę doktorską wyniki badań stanowią rozszerzenie dotychczasowej wiedzy na temat nowych parametrów biochemicznych i neuroobrazowych w badaniach celujących w opracowanie precyzyjniejszych metod stratyfikowania ryzyka powikłań krwotocznych leczenia IVT, szacowania rokowania tkankowego i odległego rokowania klinicznego u pacjentów z OUNM.

Przedstawione w pracach wyniki, jakkolwiek obarczone ograniczeniami metodologicznymi - w dużej mierze związanymi z charakterystyką badanej choroby (prace projektowe nie mogą opóźniać rutynowego postępowania diagnostyczno-terapeutycznego) wnoszą istotne dane do dalszych prac nad stworzeniem optymalnego modelu predykcji ryzyka powikłań krwotocznych i szacowania rokowania tkankowego oraz definiują potencjalnie najbardziej efektywne kierunki dalszych badań w tym zakresie.

STRESZCZENIE

Leczenie IVT przy użyciu rtPA jest obok trombektomii mechanicznej podstawową metodą terapii rekanalizacyjno-reperfuzyjnej OUNM. W ostatnich latach dokonał się dynamiczny postęp w zakresie możliwości logistycznych i medycznych stosowania leczenia rekanalizacyjno-reperfuzyjnego, ze wzrastającą liczbą wykonywanych procedur i odsetkiem tak leczonych pacjentów, a także rozwojem i poprawą dostępności zaawansowanych metod neuroobrazowania.

Myślą przewodnią mojej rozprawy doktorskiej jest złożona charakterystyka czynników wpływających na rokowanie pacjenta po udarze niedokrwiennym mózgu, w tym na tzw. rokowanie tkankowe. W pracach cyklu zwrócono uwagę, że rokowanie tkankowe uzależnione jest nie tylko od parametrów wynikających z zaburzeń perfuzji mózgowej, ale również od innych czynników – konstytutywnych, wyeksponowanych w pracy poglądowej oraz potencjalnie modyfikowalnych, w tym takich, które prowadzą do wtórnego ukrwotocznienia.

W pracy poglądowej „The salvageable brain in acute ischemic stroke. The concept of a reverse mismatch: a mini-review. Metab Brain Dis." wprowadzono pojęcie „odwróconego mismatchu" (reverse mismatch) – niedopasowania pomiędzy sekwencjami DWI i T2W/FLAIR, perfuzyjnymi i DWI, DWI wyjściowym i DWI kontrolnym, które jest manifestacją nierzadko obserwowanego w klinice zjawiska - odmiennego rokowania tkankowego pomimo „podobnych" podstawowych parametrów wyjściowych (właściwości perfuzyjne, wydolność układu sercowo-naczyniowego, powikłania – m.in. infekcje), co niejako potwierdza, że na rokowanie tkankowe wpływają, oprócz ww., również inne czynniki – biochemiczne, genetyczne.

Pomimo prawidłowej kwalifikacji do IVT (rezygnacja u pacjentów z istotnymi zdefiniowanymi czynnikami ryzyka), część chorych rozwija powikłania krwotoczne, w tym sICH, co dotyczy 3-7% pacjentów i wiąże się z gorszym 90-dniowym rokowaniem (stan funkcjonalny) i wyższym odsetkiem niepełnosprawności niż u pacjentów nieleczonych. Dotychczas wykorzystywane systemy stratyfikujące ryzyko transformacji krwotocznej po leczeniu IVT wykazują jedynie umiarkowaną wartość predykcyjną i choć częściowo użyteczne w praktyce klinicznej, wymagają doskonalenia, to jest powiększenia mocy predykcyjnej w kontekście ryzyka wtórnego ukrwotocznienia, w tym identyfikacji i włączenia do dotychczasowych modeli nowych parametrów. Takimi parametrami mogą być mikrokrwawienia mózgowe albo bieżące szeroko pojęte złożone zmiany biochemiczne krwi obwodowej wpływające na jej parametry reologiczne.

W kontynuacji tych rozważań, celem mojej pracy doktorskiej było empiryczne sprawdzenie następujących hipotez:

- u pacjentów z OUNM wyjściowa obecność mikrokrwawień mózgowych zwiększa ryzyko śródczaszkowych powikłań krwotocznych w przypadku zastosowania leczenia trombolitycznego i może być dodatkowym czynnikiem w szacowaniu ryzyka tych powikłań
- u pacjentów z OUNM stężenia niektórych białek krwi obwodowej przed leczeniem trombolitycznym – pojedynczych bądź w bardziej złożonych wzorach – związane jest z ryzykiem śródczaszkowych powikłań krwotocznych wtórnych do takiej terapii

Do badań włączono pacjentów Kliniki Neurologii Dorosłych Gdańskiego Uniwersytetu Medycznego / Uniwersyteckiego Centrum Klinicznego w Gdańsku z rozpoznaniem OUNM, zakwalifikowanych do leczenia IVT pomiędzy 20.03.2019 a 19.10.2020. Badania MRI mózgowia zostały przeprowadzone na aparacie 1.5 T Siemens Magnetom Aera system. Badanie wyjściowe MRI, przed podażą rtPA, wykonywano według protokołu GoBrain (sekwencje: T1 GRE, TSE, FLAIR, DWI, T2*-EPI) - protokół skrócony, dedykowany pacjentom w ostrej fazie OUNM z czasem akwizycji obrazów – 5.5 min, zaś badanie kontrolne w 7-9 dobie hospitalizacji w pełnym protokole (sekwencje: T1 GRE, TSE, FLAIR, DWI, T2*-EPI, DTI, SWI). Ponadto, w 22-36 godz. od rozpoczęcia leczenia IVT każdorazowo badanie kontrolne ncCT z oceną pod kątem transformacji krwotocznej.

Do oceny liczby CMBs wykorzystano sekwencję T2*-EPI, a w przypadkach wątpliwych SWI (susceptibility weighted imaging). Sekwencja T2*-EPI jest znacznie krótsza, jednak mniej czuła niż SWI w kontekście wykrywania CMBs. Wystąpienie transformacji krwotocznej po leczeniu IVT było oceniane zgodnie z klasyfikacją ECASS-II, zaś sICH definiowano według kryteriów rejestru SITS-MOST (The Safe Implementation of Thrombolysis in Stroke- Monitoring Study).

W pracy „New remote cerebral microbleeds on T2*-Weighted Echo Planar Magnetic Resonance Imaging after intravenous thrombolysis for acute ischemic stroke" wykazano, że występowanie wyjściowo CMBs jest niezależnym czynnikiem ryzyka powstawania nowych CMBs po leczeniu IVT (Risk Ratio 5.95, 95% przedział ufności 2.69-13.20, $p<0.001$), natomiast nie wykazano istotnej statystycznie korelacji pomiędzy wyjściowo stwierdzanymi CMBs a ryzykiem transformacji krwotocznej ($p=0.647$). Wydaje się, że powstawanie nowych CMBs po leczeniu IVT może nieść odległe implikacje kliniczne, w tym w kontekście ryzyka rozwoju zaburzeń funkcji poznawczych, ale na tym etapie związek ten należy traktować wyłącznie jako hipotezę popartą przesłankami, która wymaga dalszych badań.

W pracy „SWATH-MS for prospective identification of protein blood biomarkers of rtPA-associated intracranial hemorrhage in acute ischemic stroke: a pilot study" sprawdzono hipotezę, że u pacjentów z OUNM zwiększone bądź zmniejszone stężenie niektórych białek i peptydów krwi obwodowej przed leczeniem trombolitycznym zwiększa ryzyko śródczaszkowych powikłań krwotocznych takiej terapii. Zidentyfikowano 15 różnych białek (osiem w surowicy, siedem w osoczu), których stężenie różniło się w sposób istotny statystycznie, $p<0.05$, w zależności od tego czy doszło do badanego powikłania.

Uzyskane w cyklu prac składających się na rozprawę doktorską wyniki badań stanowią rozszerzenie dotychczasowej wiedzy na temat nowych parametrów neuroobrazowych i biochemicznych w badaniach celujących w opracowanie precyzyjniejszych metod stratyfikowania ryzyka powikłań krwotocznych leczenia IVT, szacowania rokowania tkankowego i odległego rokowania klinicznego u pacjentów z OUNM.

SUMMARY

IVT with rtPA and mechanical thrombectomy are mainstay of specific, recanalization-reperfusion therapies for AIS. Recent years, we observe dynamic progress in medical and logistic possibilities of applying recanalization-reperfusion therapies with significant increase in numbers of performed procedures in stroke victims, mainly because of better access to advanced neuroimaging techniques.

The keynote of my doctoral thesis is complex analysis of multiple factors that modify the functional and the tissue outcome after AIS. It is worth noting that the tissue outcome is related not only to the level of the tissue perfusion deficit but also to constitutive or potentially modifiable factors, that might also lead to secondary hemorrhage, what is discussed in the paper „The salvageable brain in acute ischemic stroke. The concept of a reverse mismatch: a mini-review. Metab Brain Dis."

We introduce the concept of reverse mismatch phenomenon - a reverse DWI - T2W/FLAIR, a reverse perfusion - DWI, or a reverse DWI-DWI (follow-up), what might be responsible for the different tissue outcome in patients exposed to similarly characterized focal brain ischemia – similar initial perfusion deficit, similar cardiovascular parameteres, with no confounders like infections. It is the confirmation that the final extent of the brain damage following AIS is shaped by multiple factors including those directly unrelated to critical hypoperfusion, eg, polymorphisms of genes or biochemical factors.

Still, despite of knowledge about risk factors, and after detailed assessment of the inclusion/exclusion criteria to IVT, the substantial portion of cases will be complicated by post-rtPA secondary hemorrhage including sICH, which occurs in 3-7 percent of cases and is associated with worse 90-day functional outcome and higher disability than in those untreated. Previously used tools and scoring systems for the assessment of the risk of IVT-associated secondary hemorrhage are based on clinical parameteres and perform poorly with only modest predictive value.

It is important challenge to find a method of the powerful identification of patients at highest risk of IVT-associated hemorrhagic transformation using new neuroimaging or biochemical parameteres like CMBs and some biochemical biomarkers affecting blood rheological properties.

The aim of this dissertation is to evaluate the thesis:

- in patients with AIS, the presence of baseline CMBs increase the risk of IVT-related secondary hemorrhage, and that baseline CMBs might be a new neuroimaging parameter for prospective assessment of that risk
- it is hypothesized that in patients with AIS any change in peptide/protein concentration before rtPA administration might potentially increase the risk of IVT-related secondary hemorrhage

In our study, we enrolled adult patients with AIS treated with rtPA, hospitalized at the Stroke Unit of the Department of Adult Neurology, University Clinical Center, Medical University of Gdansk, Poland, between March 20, 2019 and October 19, 2020.

All magnetic resonance imaging (MRI) examinations were performed with a 1.5-T MRI scanner Siemens Magnetom Aera system. The study protocol included the baseline head MRI the "Go-Brain" protocol (T1 GRE, TSE, FLAIR, DWI, T2*-EPI sequences) - designed for the fast imaging in the acute phase of stroke with acquisition time of 5.5 min. Follow-up neuroimaging studies with ncCT were performed 22-36 hours after IVT bolus and follow up MRI (complete protocol) on 7–9 days after stroke onset. The MRI axial T2∗-weighted EPI-GRE sequences were used to assess the number of CMBs. T2∗EPI-GRE sequence is much shorter but less sensitive than SWI for CMBs detection. To support the lower sensitivity of T2∗EPI-GRE sequences, SWI sequences were additionally used to confirm the CMB assessments. Hemorrhagic transformation was assessed according to ECASS-II (European Cooperative Acute Stroke Study) classification. sICH was defined according to SITS-MOST registry criteria.

„New remote cerebral microbleeds on T2*-Weighted Echo Planar Magnetic Resonance Imaging after intravenous thrombolysis for acute ischemic stroke", results: the presence of baseline CMBs correlated with a higher risk of new CMBs formation after IVT treatment (risk ratio 5.95, 95% confidence interval CI 2.69–13.20, $p < 0.001$), independently of other factors. We did not find significant correlation between baseline CMBs and the risk of hemorrhagic transformation ($p = 0.647$). It seems that the formation of new CMBs after IVT treatment might be connected with some clinical implications including cognitive decline, but further studies are warranted to investigate this hypothesis.

In publication „SWATH-MS for prospective identification of protein blood biomarkers of rtPA-associated intracranial hemorrhage in acute ischemic stroke: a pilot study" we tested the hypothesis that in patients with AIS any change in peptide/protein concentration before rtPA administration might potentially increase the risk of IVT-related secondary hemorrhage. Any changes in protein concentrations with p value < 0.05 were considered significant. We demonstrated that pre-IVT blood profiles of 15 proteins differ depending on whether the patients develop rtPA-associated secondary hemorrhage.

Presented studies are the extension of expertise in the attempt to find a better model of the powerful identification of patients at risk of rtPA-related secondary hemorrhage, and the assessment of tissue outcome, using new neuroimaging and biochemical parameteres, in patients with AIS.

BIBLIOGRAFIA

1. GBD 2019 Stroke Collaborators. Global, regional, and national burden of stroke and its risk factors, 1990-2019: a systematic analysis for the Global Burden of Disease Study 2019. Lancet Neurol. 2021 Oct;20(10):795-820. doi: 10.1016/S1474-4422(21)00252-0. Epub 2021 Sep 3. PMID: 34487721; PMCID: PMC8443449.

2. NFZ o zdrowiu. Udar niedokrwienny mózgu. 2019. https://ezdrowie.gov.pl/portal/home/zdrowe-dane/raporty/nfz-o-zdrowiu-udar-niedokrwienny-mozgu

3. Emberson J, Lees KR, Lyden P, Blackwell L, Albers G, Bluhmki E, Brott T, Cohen G, Davis S, Donnan G, Grotta J, Howard G, Kaste M, Koga M, von Kummer R, Lansberg M, Lindley RI, Murray G, Olivot JM, Parsons M, Tilley B, Toni D, Toyoda K, Wahlgren N, Wardlaw J, Whiteley W, del Zoppo GJ, Baigent C, Sandercock P, Hacke W; Stroke Thrombolysis Trialists' Collaborative Group. Effect of treatment delay, age, and stroke severity on the effects of intravenous thrombolysis with alteplase for acute ischaemic stroke: a meta-analysis of individual patient data from randomised trials. Lancet. 2014 Nov 29;384(9958):1929-35. doi: 10.1016/S0140-6736(14)60584-5. Epub 2014 Aug 5. PMID: 25106063; PMCID: PMC4441266.

4. Goyal M, Menon BK, van Zwam WH, Dippel DW, Mitchell PJ, Demchuk AM, Dávalos A, Majoie CB, van der Lugt A, de Miquel MA, Donnan GA, Roos YB, Bonafe A, Jahan R, Diener HC, van den Berg LA, Levy EI, Berkhemer OA, Pereira VM, Rempel J, Millán M, Davis SM, Roy D, Thornton J, Román LS, Ribó M, Beumer D, Stouch B, Brown S, Campbell BC, van Oostenbrugge RJ, Saver JL, Hill MD, Jovin TG; HERMES collaborators. Endovascular thrombectomy after large-vessel ischaemic stroke: a meta-analysis of individual patient data from five randomised trials. Lancet. 2016 Apr 23;387(10029):1723-31. doi: 10.1016/S0140-6736(16)00163-X. Epub 2016 Feb 18. PMID: 26898852.

5. Karaszewski B, Wyszomirski A, Jabłoński B, Werring DJ, Tomaka D. Efficacy and Safety of Intravenous rtPA in Ischemic Strokes Due to Small-Vessel Occlusion: Systematic Review and Meta-Analysis. Transl Stroke Res. 2021 Jun;12(3):406-415. doi: 10.1007/s12975-021-00890-9. Epub 2021 Feb 28. PMID: 33641037; PMCID: PMC8055574.

6. Khatri P, Kleindorfer DO, Devlin T, Sawyer RN Jr, Starr M, Mejilla J, Broderick J, Chatterjee A, Jauch EC, Levine SR, Romano JG, Saver JL, Vagal A, Purdon B, Devenport J, Pavlov A, Yeatts SD; PRISMS Investigators. Effect of Alteplase vs Aspirin on Functional Outcome for Patients With Acute Ischemic Stroke and Minor Nondisabling Neurologic Deficits: The PRISMS Randomized Clinical Trial. JAMA. 2018 Jul 10;320(2):156-166. doi: 10.1001/jama.2018.8496. PMID: 29998337; PMCID: PMC6583516.

7. Thomalla G, Simonsen CZ, Boutitie F, Andersen G, Berthezene Y, Cheng B, Cheripelli B, Cho TH, Fazekas F, Fiehler J, Ford I, Galinovic I, Gellissen S, Golsari A, Gregori J, Günther M, Guibernau J, Häusler KG, Hennerici M, Kemmling A, Marstrand J, Modrau B, Neeb L, Perez de la Ossa N, Puig J, Ringleb P, Roy P, Scheel E, Schonewille W, Serena J, Sunaert S, Villringer K, Wouters A, Thijs V, Ebinger M, Endres M, Fiebach JB, Lemmens R, Muir KW, Nighoghossian N, Pedraza S, Gerloff C; WAKE-UP Investigators. MRI-Guided Thrombolysis for Stroke with Unknown Time of Onset. N Engl J Med. 2018 Aug 16;379(7):611-622. doi: 10.1056/NEJMoa1804355. Epub 2018 May 16. PMID: 29766770.

8. Campbell BCV, Ma H, Ringleb PA, Parsons MW, Churilov L, Bendszus M, Levi CR, Hsu C, Kleinig TJ, Fatar M, Leys D, Molina C, Wijeratne T, Curtze S, Dewey HM, Barber PA, Butcher KS, De Silva DA, Bladin CF, Yassi N, Pfaff JAR, Sharma G, Bivard A, Desmond PM, Schwab S, Schellinger PD, Yan B, Mitchell PJ, Serena J, Toni D, Thijs V, Hacke W, Davis SM, Donnan GA; EXTEND, ECASS-4, and EPITHET Investigators. Extending thrombolysis to 4·5-9 h and wake-up stroke using perfusion imaging: a systematic review and meta-analysis of individual patient data. Lancet. 2019 Jul 13;394(10193):139-147. doi: 10.1016/S0140-6736(19)31053-0. Epub 2019 May 22. Erratum in: Lancet. 2020 Jun 20;395(10241):1906. PMID: 31128925.

9. Nogueira RG, Jadhav AP, Haussen DC, Bonafe A, Budzik RF, Bhuva P, Yavagal DR, Ribo M, Cognard C, Hanel RA, Sila CA, Hassan AE, Millan M, Levy EI, Mitchell P, Chen M, English JD, Shah QA, Silver FL, Pereira VM, Mehta BP, Baxter BW, Abraham MG, Cardona P, Veznedaroglu E, Hellinger FR, Feng L, Kirmani JF, Lopes DK, Jankowitz BT, Frankel MR, Costalat V, Vora NA, Yoo AJ, Malik AM, Furlan AJ, Rubiera M, Aghaebrahim A, Olivot JM, Tekle WG, Shields R, Graves T, Lewis RJ, Smith WS, Liebeskind DS, Saver JL, Jovin TG; DAWN Trial Investigators. Thrombectomy 6 to 24 Hours after Stroke with a Mismatch between Deficit and Infarct. N Engl J Med. 2018 Jan 4;378(1):11-21. doi: 10.1056/NEJMoa1706442. Epub 2017 Nov 11. PMID: 29129157.

10. Albers GW, Marks MP, Kemp S, et al. Thrombectomy for Stroke at 6 to 16 Hours with Selection by Perfusion Imaging. *N Engl J Med*. 2018;378(8):708-718.

11. Shimosegawa E, Hatazawa J, Ibaraki M, Toyoshima H, Suzuki A. Metabolic penumbra of acute brain infarction: a correlation with infarct growth. *Ann Neurol*. 2005;57(4):495-504.

12. Amantea D, Bagetta G. Excitatory and inhibitory amino acid neurotransmitters in stroke: from neurotoxicity to ischemic tolerance. Curr Opin Pharmacol. 2017;35:111-119.

13. Fedorovich SV, Waseem TV. Metabolic regulation of synaptic activity. Rev Neurosci. 2018;29(8):825-835.

14. Wang SW, Liu Z, Shi ZS. Non-Coding RNA in Acute Ischemic Stroke: Mechanisms, Biomarkers and Therapeutic Targets. Cell Transplant. 2018;27(12):1763-1777.

15. Wang P, Shao BZ, Deng Z, Chen S, Yue Z, Miao CY. Autophagy in ischemic stroke. Prog Neurobiol. 2018;163-164:98-117.

16. Karaszewski B, Jabłoński B, Żukowicz W. The salvageable brain in acute ischemic stroke. The concept of a reverse mismatch: a mini-review. *Metab Brain Dis*. 2019;35(2):237-240.

17. Stevens SL, Vartanian KB, Stenzel-Poore MP. Reprogramming the response to stroke by preconditioning. Stroke. 2014;45(8):2527-2531.

18. Jiang T, Yu JT, Zhu XC, et al. Ischemic preconditioning provides neuroprotection by induction of AMP-activated protein kinase-dependent autophagy in a rat model of ischemic stroke. Mol Neurobiol. 2015;51(1):220-229.

19. Karaszewski B, Thomas RG, Chappell FM, et al. Brain choline concentration. Early quantitative marker of ischemia and infarct expansion?. Neurology. 2010;75(10):850-856.

20. Wahlgren N, Ahmed N, Dávalos A, et al. Thrombolysis with alteplase for acute ischaemic stroke in the Safe Implementation of Thrombolysis in Stroke-Monitoring Study (SITS-MOST): an observational study [published correction appears in Lancet. 2007 Mar 10;369(9564):826]. Lancet. 2007;369(9558):275-282.

21. Strbian D, Sairanen T, Meretoja A, et al. Patient outcomes from symptomatic intracerebral hemorrhage after stroke thrombolysis. *Neurology*. 2011;77(4):341-348.

22. Hacke W, Kaste M, Fieschi C, et al. Intravenous thrombolysis with recombinant tissue plasminogen activator for acute hemispheric stroke. The European Cooperative Acute Stroke Study (ECASS). JAMA. 1995;274(13):1017-1025.

23. Whiteley WN, Emberson J, Lees KR, et al. Risk of intracerebral haemorrhage with alteplase after acute ischaemic stroke: a secondary analysis of an individual patient data meta-analysis. *Lancet Neurol*. 2016;15(9):925-933.

24. Charidimou A, Werring D. Cerebral microbleeds: detection, mechanisms and clinical challenges. Future Neurology, 2011;6(5), 587–611.

25. Greenberg SM, Vernooij MW, Cordonnier C, et al. Cerebral microbleeds: a guide to detection and interpretation. *Lancet Neurol*. 2009;8(2):165-174.

26. Wardlaw JM, Smith EE, Biessels GJ, et al. Neuroimaging standards for research into small vessel disease and its contribution to ageing and neurodegeneration. *Lancet Neurol*. 2013;12(8):822-838.

27. Lee J, Sohn EH, Oh E, Lee AY. Characteristics of Cerebral Microbleeds. Dement Neurocogn Disord. 2018;17(3):73-82. doi:10.12779/dnd.2018.17.3.73.

28. Poels MM, Vernooij MW, Ikram MA, et al. Prevalence and risk factors of cerebral microbleeds: an update of the Rotterdam scan study. Stroke. 2010;41(10 Suppl):S103-S106. doi:10.1161/STROKEAHA.110.595181.

29. Yatawara C, Guevarra AC, Ng KP, Chander R, Lam BYK, Wong A, Mok V, Kandiah N. The role of cerebral microbleeds in the incidence of post-stroke dementia. J Neurol Sci. 2020 May 15;412:116736. doi: 10.1016/j.jns.2020.116736. Epub 2020 Feb 15. PMID: 32088471.

30. Wilson D, Ambler G, Lee KJ, et al. Cerebral microbleeds and stroke risk after ischaemic stroke or transient ischaemic attack: a pooled analysis of individual patient data from cohort studies [published correction appears in Lancet Neurol. 2019 Sep;18(9):e8] [published correction appears in Lancet Neurol. 2020 Feb;19(2):e2]. Lancet Neurol. 2019;18(7):653-665. doi:10.1016/S1474-4422(19)30197-8

31. Best JG, Ambler G, Wilson D, et al. Development of imaging-based risk scores for prediction of intracranial haemorrhage and ischaemic stroke in patients taking antithrombotic therapy after ischaemic stroke or transient ischaemic attack: a pooled analysis of individual patient data from cohort studies. Lancet Neurol. 2021;20(4):294-303. doi:10.1016/S1474-4422(21)00024-7

32. Pisters R, Lane DA, Nieuwlaat R, de Vos CB, Crijns HJ, Lip GY. A novel user-friendly score (HAS-BLED) to assess 1-year risk of major bleeding in patients with atrial fibrillation: the Euro Heart Survey. Chest. 2010;138(5):1093-1100. doi:10.1378/chest.10-0134

33. Jeon SB, Kwon SU, Cho AH, Yun SC, Kim JS, Kang DW. Rapid appearance of new cerebral microbleeds after acute ischemic stroke. Neurology. 2009;73(20):1638-1644. doi:10.1212/WNL.0b013e3181bd110f

34. Kimura K, Aoki J, Shibazaki K, Saji N, Uemura J, Sakamoto Y. New appearance of extraischemic microbleeds on T2*-weighted magnetic resonance imaging 24 hours after tissue-type plasminogen activator administration. Stroke. 2013;44(10):2776-2781. doi:10.1161/STROKEAHA.113.001778

35. Yan S, Chen Y, Zhang X, Liebeskind DS, Lou M. New microbleeds after thrombolysis: contiguous thin-slice 3T MRI. Medicine. 2014 Oct;93(20):e99. DOI: 10.1097/md.0000000000000099

36. Braemswig, Tim Bastian et al. Predictors of new remote cerebral microbleeds after IV thrombolysis for ischemic stroke. Neurology vol. 92,7 (2019): e630-e638.

37. Miwa K, Koga M, Inoue M, et al. Cerebral microbleeds development after stroke thrombolysis: A secondary analysis of the THAWS randomized clinical trial [published online ahead of print, 2021 Aug 3]. Int J Stroke. 2021;17474930211035023. doi:10.1177/17474930211035023

38. Capuana ML, Lorenzano S, Caselli MC, Paciaroni M, Toni D. Hemorrhagic risk after intravenous thrombolysis for ischemic stroke in patients with cerebral microbleeds and white matter disease. Neurol Sci. 2021;42(5):1969-1976. doi:10.1007/s10072-020-04720-y

39. Karaszewski B, Houlden H, Smith EE, et al. What causes intracerebral bleeding after thrombolysis for acute ischaemic stroke? Recent insights into mechanisms and potential biomarkers. J Neurol Neurosurg Psychiatry. 2015;86(10):1127-1136. doi:10.1136/jnnp-2014-309705

40. Rapalino, O., Heberlein, K. & Ph, D. New Strategies for Protocol Optimization for Clinical MRI : Rapid Examinations and Improved Patient Care. Siemens Magnetom 22–25 (2016).

41. Fazekas F, Chawluk JB, Alavi A, Hurtig HI, Zimmerman RA. MR signal abnormalities at 1.5 T in Alzheimer's dementia and normal aging. *AJR Am J Roentgenol*. 1987;149(2):351-356.

42. Charidimou A, Kakar P, Fox Z, Werring DJ. Cerebral microbleeds and recurrent stroke risk: systematic review and meta-analysis of prospective ischemic stroke and transient ischemic attack cohorts. Stroke. (2013) 44:995– 1001.

PUBLIKACJE WŁĄCZONE DO PRACY DOKTORSKIEJ

1. Karaszewski B, Jabłoński B, Żukowicz W. The salvageable brain in acute ischemic stroke. The concept of a reverse mismatch: a mini-review. Metab Brain Dis. 2020 Feb;35(2):237-240.
   doi: 10.1007/s11011-019-00517-x.
   Punktacja IF: 3.584
   Punktacja MEiN: 70.000

2. Jabłoński B, Gójska-Grymajło A, Ossowska D, Szurowska E, Wyszomirski A, Rojek B, Karaszewski B. New remote cerebral microbleeds on T2*-Weighted Echo Planar Magnetic Resonance Imaging after intravenous thrombolysis for acute ischemic stroke. Frontiers in Neurology. 2022;12:744701.
   Published 2022 Feb 15.
   doi: 10.3389/fneur.2021.744701
   Punktacja IF: 4.003
   Punktacja MEiN: 100.000

3. Karaszewski B, Gójska-Grymajło A, Czaplewska P, Jabłoński B, Lewandowska AE, Ossowska D, Wyszomirski A, Hałas M, Szurowska E. SWATH-MS for prospective identification of protein blood biomarkers of rtPA-associated intracranial hemorrhage in acute ischemic stroke: a pilot study. Sci Rep. 2021 Sep 21;11(1):18765.
   doi: 10.1038/s41598-021-97710-9.
   Punktacja IF: 4.380
   Punktacja MEiN: 140.000

Całkowita punktacja IF: 11.967
Całkowita punktacja MEiN: 310.000

Metabolic Brain Disease (2020) 35:237–240
https://doi.org/10.1007/s11011-019-00517-x

REVIEW ARTICLE

The salvageable brain in acute ischemic stroke. The concept of a reverse mismatch: a mini-review

Bartosz Karaszewski [1,2,3] · Bartosz Jabłoński [1,2] · Wioletta Żukowicz [1,2]

Received: 26 September 2019 / Accepted: 14 November 2019 / Published online: 20 December 2019

Abstract
Recent studies have opened a new era in treatment of acute ischemic stroke, enabling thrombolysis or thrombectomy far beyond the standard therapeutic "time windows". These therapeutic protocols are built on various combinations of perfusion parameters, lesion volume, and neurological assessment. However, on top of the brain perfusion, there are other multiple factors that might modify the probability of neuronal apoptosis and necrosis following focal cerebral ischemia. We hypothesize that a diagnostic approach with measurements of selected biochemical parameters in the brain, in addition to those based solely on perfusion or MR diffusion, might allow for more personalized management protocols. Moreover, some local processes in the brain, triggered by acute ischemia or its consequences other than hypoperfusion directly, like, for example, excitotoxicity, might lead to apoptosis of the cells in the brain localized also beyond the area of hypoperfusion. This phenomenon might be responsible for the expansion of the brain damage much beyond the initial perfusion deficit or beyond the initial diffusion (DWI) restriction area, reported for example in T2W or FLAIR MRI in some stroke patients who have no other reasons to deteriorate (a reverse DWI – T2W / FLAIR, a reverse perfusion – DWI, or a reverse DWI – DWI mismatch).

Keywords Ischemic stroke · Perfusion · Brain metabolism · Thrombolysis · Thrombectomy · Neuroimaging

Recanalization-reperfusion therapies for acute ischemic stroke (thrombolysis and thrombectomy), combined with other management steps, have largely improved outcome of victims of the disorder. Recent studies, based on a much more personalized therapeutic approach, have opened a new era in stroke management: Table 1 (Nogueira et al. 2017; Albers et al. 2018) and Table 2 (Thomalla et al. 2018; Ma et al. 2019).

For example, patients with a large mismatch between volumes of critical versus relative brain perfusion deficit (the whole area of hypoperfusion is much larger than core hypoperfusion) might be effectively treated with thrombectomy far beyond the standard therapeutic time window (Albers et al. 2018; Fig. 1).

✉ Bartosz Karaszewski
bartosz@karaszewski.org

[1] Department (Chair) of Neurology, Medical University of Gdansk, Gdansk, Poland

[2] Department of Adult Neurology, Medical University of Gdansk and University Clinical Center in Gdansk, ul. Dębinki 7, 80-952 Gdańsk, Poland

[3] The Main Expert in Stroke Medicine for the Polish Ministry of Health, Warsaw, Poland

These current protocols of the personalized treatment with thrombolysis and thrombectomy are built solely on various combinations of perfusion parameters (cerebral blood volume or cerebral blood flow or mean transit time), lesion volume, and neurological dysfunction in the clinical assessment (Nogueira et al. 2017; Albers et al. 2018; Thomalla et al. 2018; Ma et al. 2019). The level of tissue perfusion deficit in acute ischemic stroke obviously correlates with the likelihood of tissue death, probably much stronger than most other known characteristics (Shimosegawa et al. 2005; Chan et al. 2016). However, on top of the brain perfusion, there are other multiple factors that might modify the probability of neuronal apoptosis and necrosis following focal cerebral ischemia. These include individual variability in excitotoxicity, polymorphisms of genes of enzymes involved in energy metabolism processes, variability in mechanisms of Ca^{2+} cell entry, polymorphisms of protein peptide components of selected receptors like NMDA (N-methyl-D-aspartate) or AMPA (α-amino-3-hydroxy-5-methyl-4-isoxazolepropionic acid) ones, polymorphisms of Bcl-2 interacting domain (BID) and other proapoptotic proteins, multiple factors stimulating or inhibiting apoptotic pathways, local regulatory mechanisms of reactive oxygen species (ROS) production and release,

Table 1 Treatment of acute ischemic stroke with mechanical thrombectomy beyond standard "time window" (Nogueira et al. 2017; Albers et al. 2018)

Trial	DAWN	DEFUSE-3
Number of participants	206	182
Last known well to randomization (treatment) time [h]	6 to 24	6 to 16
Occlusion site	Intracranial internal carotid artery First segment of middle cerebral artery Second segment of middle cerebral artery	Intracranial internal carotid artery First segment of middle cerebral artery Second segment of middle cerebral artery
Main inclusion criteria	*Clinical - Core Mismatch* (MR DWI or CTP-rCBF): - ≥ 80 years of age, score of 10 or higher on the NIHSS and an "infarct" volume of less than 21 ml - < 80 years of age, score of 10 or higher on the NIHSS, and an "infarct" volume of less than 31 ml - < 80 years of age, score of 20 or higher on the NIHSS, and an infarct "volume" of 31 to less than 51 ml	*"Infarct" Core – Perfusion Mismatch* (CTP-rCBF+MTT or MRI + PWI): - initial perfusion "infarct" volume (*ischemic core*) < 70 ml - ratio of volume of ischemic tissue (Tmax >6 s) to initial perfusion "infarct" volume ≥ 1.8 - absolute volume of potentially reversible ischemia (of "penumbra") ≥ 15 ml
Results, mRS 90 d: 0–2	49 vs 13%	45 vs 17%

Abbreviations: DAWN, DWI or CTP Assessment with Clinical Mismatch in the Triage of Wake-Up and Late Presenting Strokes Undergoing Neurointervention with Trevo; DEFUSE-3, The Endovascular Therapy Following Imaging Evaluation for Ischemic Stroke; MR DWI, Magnetic Resonance Diffusion-Weighted Imaging; CTP-rCBF, Computed Tomography Perfusion-relative Cerebral Blood Flow; MTT, Mean Transit Time; Tmax, Time to maximum threshold; NIHSS, National Institutes of Health Stroke Scale; PWI, Perfusion-Weighted Imaging; mRS, modified Rankin Scale

and many others (Table 3) (Lee et al. 2000; Broughton et al. 2009; Liao et al. 2010; Zille et al. 2012; Turner et al. 2013; Baron et al. 2014; Amantea and Bagetta 2017; Ao et al. 2018; Fedorovich and Waseem 2018; Wang et al. 2018a, b;).

The variability of combinations of these factors explains why patients exposed to similarly characterized focal brain ischemia in clinical practice (eg, the same brain structures involved, similar initial volume of the lesion, perfusion deficit, collaterals, cardiovascular and autonomic nervous system sufficiency, no confounders like infections or other inflammations) might end up with different clinical and tissue outcomes (lesion volumes). For the same reasons, the time from vessel occlusion to tissue death might be different in patients with the same characteristics of perfusion deficit and vascularization. It is worth noting that these factors might be either constitutive (eg, polymorphisms of genes of enzymes involved in energy metabolism processes) or inducible (eg, the excitotoxicity) (Anderson et al. 2013; Biffi et al. 2014; Amantea and Bagetta 2017; Díaz-Maroto Cicuéndez et al. 2017). Moreover, some of them might be responsible for the so-called preconditioning phenomenon (the tissue that was exposed to minor temporary hypoperfusion in the past is more

Table 2 Treatment of acute ischemic stroke with thrombolysis beyond standard "time window" (Thomalla et al. 2018; Ma et al. 2019)

trial	WAKE-UP	EXTEND, ECASS4-EXTEND, and EPITHET, meta-analysis
Number of participants	503	414 (304 with automated perfusion mismatch)
Last known well to randomization (treatment) time [h]	wake-up strokes (also: no information about the onset of symptom – eg, aphasia, "confusion")	4.5–9.0 or wake-up strokes
Neuroimaging criteria	Mismatch between Magnetic Resonance DWI and FLAIR: - mismatch between the presence of an abnormal signal on DWI and no visible signal change on FLAIR in the area of acute ischemia	*Automated* Perfusion Mismatch (CTP-rCBF or MRI + PWI): - initial infarct volume ("ischemic core") < 70 ml - ratio of volume of ischemic tissue (Tmax >6 s) to initial "infarct" volume ≥ 1.2 - absolute volume of potentially reversible ischemia ("penumbra") ≥ 10 ml
Results, mRS 90 d: 0–1	53.3 vs 41.8%	36 vs 29%
Symptomatic intracerebral haemorrhage (PH2)	2.0 vs 0.4%	5 vs < 1%

Abbreviations: FLAIR, Fluid Attenuation Inversion Recovery; PH2, Parenchymal Haemorrhage type 2; MRI, Magnetic Resonance Imaging; CTP, Computed Tomography P*erfusion*; PWI, Perfusion-Weighted Imaging

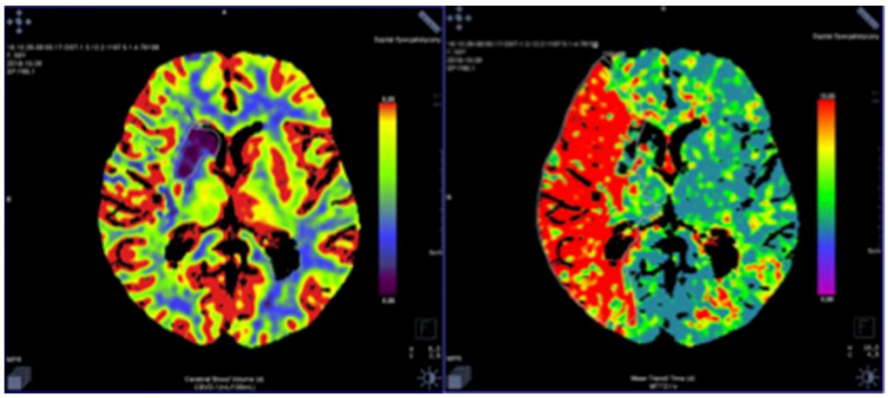

Fig. 1 Brain perfusion in computed tomography. Cerebral blood volume (CBV, left) and mean transit time (MTT, right) maps. The area of severely reduced CBF (<30% of that in normally perfused tissue) with reduced CBV represents the "ischemic core"; the region of perfusion delay of >6 s represents the "hypoperfused tissue". Subtraction of the two represents "penumbra" (from The University Clinical Center and The Medical University of Gdansk imaging databases)

likely to end up with a better "outcome" after severe ischemia) (Stevens et al. 2014; Jiang et al. 2015).

Taking the above, we hypothesize that a diagnostic approach with measurements of selected biochemical parameters in the brain, in addition to those based solely on perfusion or MR diffusion, might allow for more personalized management protocols than those used currently. For example, because the volume of the DWI (Diffusion-Weighted Imaging) lesion in ischemic stroke patients who have higher choline concentrations immediately outside the lesion is more likely to further expand, the information on the choline concentration – measurable in the early phase of stroke with proton MR spectroscopy – might be used to specify some therapeutic decisions (Karaszewski et al. 2010).

Table 3 Factors that might modify the probability of neuronal apoptosis and necrosis following focal cerebral ischemia

Factors that might modify the probability of neuronal death
multiple factors stimulating or inhibiting apoptotic pathways
enhancement of ischemic neuronal death by mitogen-activated protein (MAP) kinases involved
polymorphisms of Bcl-2 interacting domain (BID) and other proapoptoticproteins
polymorphisms of genes of enzymes involved in energy metabolism processes
individual variability in excitotoxicity
polymorphisms of protein peptide components of selected receptors like NMDA or AMPA
toxicity of glutamate
variability in mechanisms of Ca2+ cell entry
Zn^{2+} overload and toxicity
enhancement of neuronal excitotoxicity by protein kinase C (PKC)
changes in *dopamine concentration*
local regulatory mechanisms of reactive oxygen species (ROS) production and release
neuroprotection of several neurotransmitters such as serotonin, adenosine and γ-aminobutyric acid
reduction of brain damage by growth factors including IGF-1, neurotrophins 4/5 (NT-4/5), brain-derived neurotrophic factor (BDNF), nerve growth factor (NGF), basic fibroblast growth factor
reactions after postischemic reperfusion
inflammatory cascade

Importantly, some local processes in the brain, triggered by acute ischemia or its consequences other than hypoperfusion directly, like, for example, excitotoxicity, might not only stimulate already triggered pathways towards neuronal death but also lead to apoptosis of the cells in the brain localized beyond the area of hypoperfusion. This phenomenon might be responsible for the expansion of the brain damage (possibly detectable for example in the follow-up T2-Weighted or Fluid-Attenuated Inversion Recovery (FLAIR) MR imaging) much beyond the initial perfusion deficit and/or beyond the initial DWI lesion. This occurrence, observed in some stroke patients who have no other reasons to deteriorate, might be described as a reverse DWI – T2W (or FLAIR), a reverse perfusion – DWI, or a reverse DWI – (follow-up) DWI mismatch (Fig. 2).

In conclusion, the final extent of the brain damage following acute ischemic stroke is shaped by multiple factors including those directly unrelated to critical hypoperfusion. Some of these mechanisms might lead to apoptosis of the cells localized beyond the area of hypoperfusion. This phenomenon might be responsible for the expansion of the brain damage much beyond the perfusion deficit or beyond the initial DWI lesion, possibly also leading to T2-weighted (T2W) lesion volume much larger than the initial perfusion and/or diffusion restriction areas. This occurrence, observed in some stroke patients who have no other reasons to deteriorate, might be

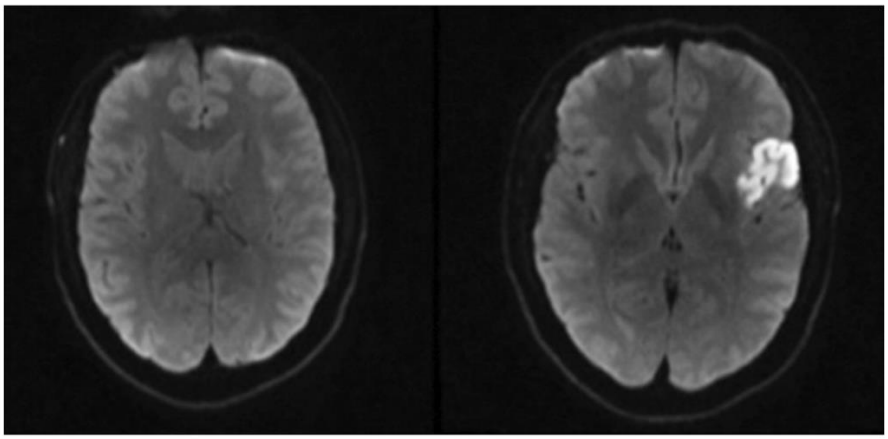

Fig. 2 Substantial expansion of the DWI lesion in a thrombolysed ischemic stroke patient between MRI at admission (short protocol) - nearly 2 h from stroke onset - and the follow-up performed 5 days later, appearing despite no clinical confounders or complications (from The University Clinical Center and The Medical University of Gdansk imaging databases)

described as a reverse DWI – T2W / FLAIR, a reverse perfusion – DWI, or a reverse DWI – DWI mismatch.

References

Albers GW, Marks MP, Kemp S, Christensen S, Tsai JP, Ortega-Gutierrez S, McTaggart R, Torbey MT, Kim-Tenser M, Leslie-Mazwi T, Sarraj A, Kasner SE, Ansari SA, Yeatts SD, Hamilton S, Mlynash M, Heit JJ, Zaharchuk G, Kim S, Carrozzella J, Palesch YY, Demchuk AM, Bammer R, Lavori PW, Broderick JP, Lansberg MG, DEFUSE 3 Investigators (2018) Thrombectomy for stroke at 6 to 16 hours with selection by perfusion imaging. N Engl J Med 378:708–718

Amantea D, Bagetta G (2017) Excitatory and inhibitory amino acid neurotransmitters in stroke: from neurotoxicity to ischemic tolerance. Curr Opin Pharmacol 35:111–119

Anderson CD, Biffi A, Nalls MA et al (2013) Common variants within oxidative phosphorylation genes influence risk of ischemic stroke and intracerebral hemorrhage. Stroke 44:612–619

Ao LY, Yan YY, Zhou L, Li CY, Li WT, Fang WR, Li YM (2018) Immune cells after ischemic stroke onset: roles, migration, and target intervention. J Mol Neurosci 66:342–355

Baron JC, Yamauchi H, Fujioka M, Endres M (2014) Selective neuronal loss in ischemic stroke and cerebrovascular disease. J Cereb Blood Flow Metab 34:2–18

Biffi A, Sabuncu MR, Desikan RS et al (2014) Genetic variation of oxidative phosphorylation genes in stroke and Alzheimer's disease. Neurobiol Aging 35:1956.e1–1956.e8

Broughton BRS, Reutens DC, Sobey C (2009) Apoptotic mechanisms after cerebral ischemia. Stroke 40:e331–e339

Chan SL, Sweet JG, Bishop N, Cipolla MJ (2016) Pial collateral reactivity during hypertension and aging: understanding the function of collaterals for stroke therapy. Stroke 47:1618–1625

Díaz-Maroto Cicuéndez I, Fernández-Díaz E, García-García J et al (2017) The UCP2-866G/A polymorphism could be considered as a genetic marker of different functional prognosis in ischemic stroke after recanalization. NeuroMolecular Med 19:571–578

Fedorovich SV, Waseem TV (2018) Metabolic regulation of synaptic activity. Rev Neurosci 29:825–835

Jiang T, Yu JT, Zhu XC, Zhang QQ, Tan MS, Cao L, Wang HF, Shi JQ, Gao L, Qin H, Zhang YD, Tan L (2015) Ischemic preconditioning provides neuroprotection by induction of AMP-activated protein kinase-dependent autophagy in a rat model of ischemic stroke. Mol Neurobiol 51:220–229

Karaszewski B, Thomas RGR, Chappell FM et al (2010) Brain choline concentration. Early quantitative marker of ischemia and infarct expansion? Neurology 75:850–856

Lee JM, Grabb MC, Zipfel GJ, Choi DW (2000) Brain tissue responses to ischemia. J Clin Investig 106:723–731

Liao Y, Kristiansen AM, Oksvold CP et al (2010) Neuronal Ca2+-activated K+ channels limit brain infarction and promote survival. PLoS One 5(12):e15601

Ma H, Campbell BCV, Parsons MW et al (2019) Thrombolysis guided by perfusion imaging up to 9 hours after onset of stroke. N Engl J Med 380:1795–1803

Nogueira RG, Jadhav AP, Haussen DC et al (2017) Thrombectomy 6 to 24 hours after stroke with a mismatch between deficit and infarct. N Engl J Med 378:11–21

Shimosegawa E, Hatazawa J, Ibaraki M et al (2005) Metabolic penumbra of acute brain infarction: a correlation with infarct growth. Ann Neurol 57:495–450

Stevens SL, Vartanian KB, Stenzel-Poore MP (2014) Reprogramming the response to stroke by preconditioning. Stroke 45:2527–2531

Thomalla G, Simonsen CZ, Boutitie F, Andersen G, Berthezene Y, Cheng B, Cheripelli B, Cho TH, Fazekas F, Fiehler J, Ford I, Galinovic I, Gellissen S, Golsari A, Gregori J, Günther M, Guibernau J, Häusler KG, Hennerici M, Kemmling A, Marstrand J, Modrau B, Neeb L, Perez de la Ossa N, Puig J, Ringleb P, Roy P, Scheel E, Schonewille W, Serena J, Sunaert S, Villringer K, Wouters A, Thijs V, Ebinger M, Endres M, Fiebach JB, Lemmens R, Muir KW, Nighoghossian N, Pedraza S, Gerloff C, WAKE-UP Investigators (2018) MRI-guided thrombolysis for stroke with unknown time of onset. N Engl J Med 379:611–622

Turner RC, Dodson SC, Rosen CL, Huber JD (2013) The science of cerebral ischemia and the quest for neuroprotection: navigating past failure to future success. J Neurosurg 118:1072–1085

Wang SW, Liu Z, Shi ZS (2018a) Non-coding RNA in acute ischemic stroke: mechanisms, biomarkers and therapeutic targets. Cell Transplant 27:1763–1777

Wang P, Shao BZ, Deng Z et al (2018b) Autophagy in ischemic stroke. Prog Neurobiol 163-164:98–117

Zille M, Farr TD, Przesdzing I, Müller J, Sommer C, Dirnagl U, Wunder A (2012) Visualizing cell death in experimental focal cerebral ischemia: promises, problems, and perspectives. J Cereb Blood Flow Metab 32:213–231

frontiers in Neurology

ORIGINAL RESEARCH
published: 15 February 2022
doi: 10.3389/fneur.2021.744701

New Remote Cerebral Microbleeds on T2*-Weighted Echo Planar MRI After Intravenous Thrombolysis for Acute Ischemic Stroke

*Bartosz Jabłoński[1], Anna Gójska-Grymajło[1], Daria Ossowska[1,2], Edyta Szurowska[2], Adam Wyszomirski[1], Bartłomiej Rojek[1] and Bartosz Karaszewski[1]**

[1] Department of Adult Neurology, University Clinical Center, Medical University of Gdańsk, Gdańsk, Poland, [2] II Department of Radiology, Medical University of Gdańsk, Department of Radiology, University Clinical Centre, Gdańsk, Poland

OPEN ACCESS

Edited by:
Marios Psychogios,
University Hospital of Basel, Switzerland

Reviewed by:
Ozge Altintas Kadirhan,
Kirklareli University, Turkey
Sheng Zhang,
Zhejiang Provincial People's Hospital, China

***Correspondence:**
Bartosz Karaszewski
bartosz@karaszewski.org

Specialty section:
This article was submitted to Stroke, a section of the journal Frontiers in Neurology

Received: 20 July 2021
Accepted: 16 December 2021
Published: 15 February 2022

Citation:
Jabłoński B, Gójska-Grymajło A, Ossowska D, Szurowska E, Wyszomirski A, Rojek B and Karaszewski B (2022) New Remote Cerebral Microbleeds on T2*-Weighted Echo Planar MRI After Intravenous Thrombolysis for Acute Ischemic Stroke. Front. Neurol. 12:744701. doi: 10.3389/fneur.2021.744701

Background: The main and well-defined complication of intravenous administration of recombinant tissue plasminogen activator (tPA) in patients with acute ischemic stroke (AIS) is symptomatic intracranial hemorrhage (sICH). However, rtPA might also be connected with the formation of cerebral microbleeds (CMBs), located remotely from the ischemic lesions, that may remain clinically silent. This association might be important because the load of CMBs has been associated with cognitive impairment. We investigated whether administration of rtPA in AIS results in the appearance of new CMBs and if the initial load of CMBs is associated with hemorrhagic transformation.

Methods: A total of fifty-nine consecutive patients with AIS treated with rtPA underwent MRI including T2*-weighted Echo Planar Imaging (T2*-EPI) shortly before and 7–9 days after rtPA administration. We calculated the load of new CMBs located outside the MR diffusion restriction area in the follow-up imaging and assessed hemorrhagic transformation with ECASS-II scoring.

Results: A total of forty-nine patients were included for the final analysis. On initial T2*-EPI-GRE, 37 baseline microbleeds (CMBs) were observed in 14 patients (28.6%). On follow-up T2*-EPI-GRE amount of CMBs increased to a total number of 103. New CMBs were found in 5 (14.3%) of 35 patients without and in 9 (64.3%) of 14 with any baseline CMBs. Multiple logistic regression analysis indicated that presence of baseline CMBs (risk ratio [RR] 5.95, 95% CI 2.69–13.20, $p < 0.001$) and lower platelets level (risk ratio [RR] 0.992, 95% CI 0.986–0.998, $p = 0.007$) were independently associated with new CMBs. The baseline load of CMBs was not associated with the risk of hemorrhagic transformation.

Conclusion: In this study, new CMBs were found in nearly 30% of patients with AIS on the 7–9 days after rtPA treatment. Baseline CMBs correlated with a higher risk of new CMBs appearing after the rtPA treatment, independently of other factors. At the same time, in our sample, baseline CMBs did not correlate with an increased

risk of hemorrhagic transformation. Since the associations between the CMBs load and cognitive impairment have already been proved, further studies are warranted to investigate possible associations between the thrombolytic treatment of patients with AIS, mainly those with baseline CMBs, and the risk of earlier cognitive decline.

Keywords: cerebral microbleeds, acute ischemic stroke, thrombolysis, hemorrhagic transformation, neuroimaging, MRI

INTRODUCTION

Intravenous thrombolysis with recombinant tissue plasminogen activator (tPA) is the mainstay therapeutic method of acute ischemic stroke (AIS) with proven clinical benefit (1) and is recommended up to 4.5 h after stroke onset (2). In addition, recent randomized controlled trials and meta-analyses enabled the extension of the time window in selected cases or administration of rtPA in some subjects with unknown onset of stroke (3–5).

The most common complication of rtPA treatment is the hemorrhagic transformation of the ischemic lesion. This transformation might be of various severity that has been classified with ECASS-II score (**Table 1**) (6). The severity of hemorrhagic transformation is strictly connected with clinical significance and the symptomatic intracerebral hemorrhage (sICH), which occurs in 3–7% of rtPA treated patients, is of the highest clinical interest since it is associated with poor functional outcomes. Symptomatic intracerebral hemorrhage has been well-characterized in the multiple studies (2, 7–9).

Administration of rtPA might also result in another hemorrhagic complication—cerebral microhemorrhages or microbleeds (CMBs). CMBs are small, rounded signal loss lesions surrounded by brain tissue with a diameter up to 5 mm. CMBs might appear remotely from the ischemic lesion in an isolated or diffuse pattern across the brain. The CMBs neuroimaging characteristics are listed in **Table 2** (10–13). The prevalence of CMBs is significantly higher in the elderly population with multiple comorbidities and high-total cardiovascular risk, especially hypertension with subsequent hypertensive arteriopathy (13, 14). Usually, CMBs are clinically silent in the terms of acute stroke care but might have a cumulative impact on patients in the following years, mainly because of the associations between the load of CMBs and cognitive impairment (15–20).

Cerebral microbleeds have also been under study because of their possible pathophysiological connection with hemorrhagic transformation as CMBs are commonly treated as markers of increased vascular vulnerability due to severe small vessel disease (21–23). This connection seems plausible also in light of the recent analyses that have revealed that CMBs burden might be a useful single marker of the risk of sICH in patients, after stroke or TIA, receiving oral anticoagulants (OACs) (24, 25). In these reports, CMBs burden was more predictive of sICH than other tools, including HAS-BLED (26).

The problem of rtPA-associated CMBs has already been addressed in a few studies (27–32). However, only four of them were planned to assess true baseline CMBs load with MRI preceding the rtPA administration (28–31). The problem to quantify and compare CMBs before and after the thrombolytic treatment is related to the fact that their proper assessment requires the use of MRI. The long duration of standard MRI testing interferes with the urge of administering the rtPA and thus precludes regular and easy use of this neuroimaging technique in thrombolysed patients.

TABLE 1 | The european cooperative acute stroke study classification of hemorrhagic transformation.

Hemorrhage classification	Radiographic appearance
Haemorrhagic infarction type 1 (HI1)	Small hyperdense petechiae.
Haemorrhagic infarction type 2 (HI2)	More confluent hyperdensity throughout the infarct zone; without mass effect.
Parenchymal hematoma type 1 (PH1)	Homogeneous hyperdensity occupying <30% of the infarct zone; some mass effect.
Parenchymal hematoma type 2 (PH2)	Homogeneous hyperdensity occupying >30% of the infarct zone; significant mass effect. Or, any homogenous hyperdensity located beyond the borders of the infarct zone.

In the presented study, we investigated whether administration of rtPA in AIS results in the appearance of new CMBs and whether the baseline CMBs load increases the risk of new CMBs and hemorrhagic transformation after the rtPA treatment. The assessment was performed using pre- and post-thrombolysis special MRI protocols.

METHODS

Patients and Study Protocol

A total of fifty-nine consecutive patients with AIS treated with intravenous thrombolysis between March 20, 2019 and October 19, 2020 were prospectively enrolled into the study. The study protocol included the following:

(1) head MRI that includes T2*-weighted Echo Planar Imaging (T2*-EPI-GRE) in the protocol before rtPA administration (to exclude ICH);
(2) intravenous thrombolysis, as the main therapy (without mechanical thrombectomy) with standard dosage of rtPA administered either within 4.5 h after stroke onset (the time when a patient was last known to be without symptoms), according to standard dosing protocol approved and recommended for thrombolysis in patients with AIS (33)

TABLE 2 | Cerebral microbleeds (CMBs)—neuroimaging characteristics.

Small, rounded signal loss lesions surrounded by brain tissue
Located outside the infarcted area
Diameter up to 5 mm
Detected on T2*-weighted and susceptibility-weighted imaging (SWI)
Blooming effect on T2*-weighted MRI
Generally not seen on computed tomography, FLAIR, T1-weighted MRI

or with unknown time of onset based on WAKE-UP trial protocol (3) with DWI-FLAIR MRI mismatch (five patients).

(3) Follow-up MRI that includes T2*-EPI-GRE in the protocol, performed on 7–9 days after stroke onset (for therapeutic reasons, in eight cases, follow-up MRI was performed out of the target time frame).

The aforementioned steps constituted the eligibility criteria—patients who could not follow one or more of the steps were not included in the assessments. In addition, the exclusion criterion was the poor quality of obtained neuroimaging data. Forty-nine patients (26 women and 23 men, mean age - 66 years) were included in the final analysis. Three of them had been treated with the non-vitamin K antagonist oral anticoagulant (NOAC) before stroke onset because of atrial fibrillation. However, their laboratory-assessed anticoagulant activity on admission was low (<20 ng/ml) and did not constitute a contraindication for thrombolysis. None of the patients involved in the analysis received any kind of anticoagulation before the follow-up MRI.

All the patients provided informed consent for the involvement in the study. The clinical characteristics of the study group are presented in **Table 3**.

MRI Protocol and Image Analysis

All MRI examinations were performed with a 1.5-T MRI scanner (Magnetom Aera, Siemens, Erlangen, Germany) with 20 channel head/neck coil in AutoCoil selection mode. Baseline MRI—the "Go-Brain" protocol—designed for the fast imaging in the acute phase of stroke (34), consisted of sagittal T1-weighted gradient recalled echo (GRE), axial T2-weighted turbo spin-echo (TSE), axial T2-weighted TSE fluid-attenuation inversion recovery (FLAIR), axial diffusion-weighted (DWI) single-shot echo-planar imaging (EPI), and axial T2*-weighted EPI-GRE. The high-diagnostic value of ultrafast sequences was presented by Prakkamakul et al. (35). The "Go-Brain" protocol included the "AutoAlign" mode, which uses anatomical landmarks for automated alignment for slice position and prevents erroneous double counting in the follow-up assessment.

The follow-up MRI protocol included axial T2*-weighted EPI-GRE sequences that were used to assess the number of CMBs. Next, where needed the susceptibility-weighted imaging (SWI) was used to confirm CMBs detected on the follow-up T2*-weighted EPI-GRE images. DWI sequence was also used to evaluate baseline (before rtPA administration) infarct volume. Axial T2 FLAIR sequence was used to assess the leukoaraiosis severity in the Fazekas scale (36). Detailed MRI parameters are listed in **Table 4**.

Cerebral microbleeds neuroimaging characteristics are listed in **Table 2** (10–13). CMBs observed in the region of the ischemic lesion were not included in the analysis. CMBs in T2*-weighted EPI-GRE sequences were manually assessed by three observers—a neurologist (BJ) and a radiologist working together with a physicist (ESz, DO). Discrepancies were resolved by consensus and by independent decisions of an experienced stroke neurologist (BK).

Hemorrhagic transformation was graded by the ECASS-II (European Cooperative Acute Stroke Study) classification (6) (**Table 1**). Symptomatic intracerebral hemorrhage was defined according to SITS-MOST (The Safe Implementation of Thrombolysis in Stroke- Monitoring Study) criteria (37): a type 2 parenchymal hemorrhage (PH2) with deterioration in the National Institutes of Health Stroke Scale (NIHSS) score of 4 points or more, or death.

Clinical Assessment

All the patients enrolled were clinically assessed by an experienced stroke neurologist and classified according to the Trial of Org 10172 in Acute Stroke Treatment (TOAST) classification (38).

Statistics

Interrater agreement for the MRI reading was evaluated using the weighted Cohen's kappa with linear weights and interpreted in the following way: 0.01–0.20 as poor agreement, 0.21–0.40 as fair agreement, 0.41–0.60 as moderate agreement, 0.61–0.80 as substantial agreement, and above 0.80 as almost perfect agreement.

The characteristics of the patients were presented according to mean and standard deviation (SD) for normally distributed continuous data, whereas non-normally distributed variables were described as quartiles; categorical variables were reported as counts and percentages. The between-group differences were evaluated using *t*-test or Mann-Whitney test for continuous data and the chi-square test or Fisher's exact test for categorical variables. The two-tailed tests were carried out at a significance level of $p \leq 0.05$. A generalized linear model assuming Poisson distribution with a log-link function was used to identify risk factors for the incidence of new CMBs. A stepwise forward selection was applied to build up a model with the lowest score of the Akaike information criterion. The final model was recalculated taking into account a robust error variance. Regression coefficients were expressed as adjusted relative risk (aRR) with a 95% CI. All the statistical analyses were performed using the R statistical package (version 3.6.3.).

RESULTS

On initial T2*-EPI-GRE we identified 37 baselines CMBs in 14 patients (28.6%). A total of thirty-four (91.9%) of CMBs were localized in the cortical/subcortical area and only 3 (8.1%) in the deep brain structures. In all but one patient, the number of baseline CMBs did not exceed 3. Interobserver agreement

TABLE 3 | Characteristics of two groups – with (*N* = 14) and without (*N* = 35) new CMBs.

	1 (*N* = 14)	0 (*N* = 35)	Total (*N* = 49)	*p* value
Age, y, median (Q1, Q3)	72.5 (66.5, 84.0)	62.0 (46.0, 75.5)	66.0 (56.0, 80.0)	**0.026**
Time from onset to treatment, min, mean (SD)	177.4 (63.3)	170.9 (59.5)	172.8 (60.0)	0.734
Hypertension	13 (92.9%)	27 (77.1%)	40 (81.6%)	0.415^{fe}
Diabetes	6 (42.9%)	11 (31.4%)	17 (34.7%)	0.448
Atrial fibrillation	4 (28.6%)	4 (11.4%)	8 (16.3%)	0.202^{fe}
Antiplatelet drugs	5 (35.7%)	15 (42.9%)	20 (40.8%)	0.646
NOAC on admission	2 (14.3%)	1 (2.9%)	3 (6.1%)	0.193^{fe}
Previous clinical stroke	3 (21.4%)	7 (20.0%)	10 (20.4%)	0.999^{fe}
Systolic blood pressure admission, mmHg, mean (SD)	164.1 (21.6)	154.5 (26.1)	157.2 (25.1)	0.226
Diastolic blood pressure admission, mmHg, mean (SD)	86.5 (15.5)	84.6 (13.7)	85.2 (14.1)	0.679
Glucose, mg/dl, median (Q1, Q3)	126.0 (104.5, 141.2)	121.0 (105.0, 142.0)	121.0 (104.0, 143.0)	0.715^{m-w}
Platelets, x10^9/l, median (Q1, Q3)	222.0 (182.5, 240.8)	234.0 (192.5, 296.5)	231.0 (182.0, 266.0)	0.250^{m-w}
Creatinine, mg/dl, mean (SD)	1.0 (0.2)	0.9 (0.2)	0.9 (0.2)	**0.035**
INR, mean (SD)	1.0 (0.1)	1.0 (0.1)	1.0 (0.1)	0.827
NIHSS score, admission, median (Q1, Q3)	5.0 (4.0, 5.8)	5.0 (3.0, 10.0)	5.0 (3.0, 7.0)	0.600^{m-w}
NIHSS score, discharge, median (Q1, Q3)	0.5 (0.0, 1.8)	1.0 (0.0, 2.0)	1.0 (0.0, 2.0)	0.698^{m-w}
TOAST classification				0.624^{fe}
LAA	2 (14.3%)	7 (20.0%)	9 (18.4%)	
CE	5 (35.7%)	6 (17.1%)	11 (22.4%)	
SVD	3 (21.4%)	9 (25.7%)	12 (24.5%)	
UE	4 (28.6%)	13 (37.1%)	17 (34.7%)	
Hemorrhagic transformation, ECASS				0.647^{fe}
HI1	3 (21.4%)	3 (8.6%)	6 (12.2%)	
HI2	1 (7.1%)	1 (2.9%)	2 (4.1%)	
NH	10 (71.4%)	29 (82.9%)	39 (79.6%)	
PH1	0 (0.0%)	1 (2.9%)	1 (2.0%)	
PH2	0 (0.0%)	1 (2.9%)	1 (2.0%)	
Baseline DWI Volume, ml, median (Q1, Q3)	2.2 (0.0, 13.4)	3.9 (0.6, 19.5)	3.4 (0.0, 16.0)	0.584^{m-w}
Periventricular and deep white matter hyperintensities [2–3 in Fazekas scale]	5 (35.7%)	8 (22.9%)	13 (26.5%)	0.357
Presence of baseline CMBs	9 (64.3%)	5 (14.3%)	14 (28.6%)	**< 0.001**

SD, standard deviation; Q1, the first quartile; Q3, the third quartile; fe, Fisher's exact test; m-w, Mann-Whitney test; ICH, intracerebral hemorrhage; TOAST, Trial of Org 10172 in Acute Stroke Treatment (classification); LAA, large-artery atherosclerosis; CE, cardioembolism, SVD, small-vessel disease; UE- stroke of undetermined etiology; ECASS, European Cooperative Acute Stroke Study (classification); NH, no hemorrhage; HI1, haemorrhagic infarction type 1; HI2, hemorrhagic infarction type 2; PH1, parenchymal hematoma type 1; PH2, parenchymal hematoma type 2; NOAC, novel oral anticoagulant; NIHSS, National Institute of Health Stroke Scale; SBP, systolic blood pressure; DBP, diastolic blood pressure; DWI, diffusion weighted imaging. Statistically significant differences between these two groups of patients are marked with bald fonts of the p-value.

TABLE 4 | MRI sequences and parameters used in the study.

Sequence	TR [ms]	TE [ms]	IT [ms]	Slices	Slice thickness [mm]	Gap [mm]	*b*-value
Sagital T1 (GRE)	595	11	-	27	5	1	-
Axial T2 (TSE)	4,700	101	-	25	5	1	-
Axial T2 FLAIR	5,500	78	1,930	25	5	1	-
Axial T2* (EPI-GRE)	6,120	75	-	25	5	1	-
Axial DWI (EPI)	4,500	89	-	31	5	0.6	0.800
3D SWI (GRE)	49	40	-	56	2	-	-

GRE, gradient recalled echo; TSE, turbo spin echo; FLAIR, fluid-attenuated inversion recovery; EPI, echo-planar imaging; DWI, diffusion-weighted imaging; SWI, susceptibility-weighted imaging.

was high and kappa values are presented in **Table 5**. On follow-up T2*-EPI-GRE, the total amount of CMBs increased up to an absolute number of 103 (all patients combined). New CMBs were found in 5 (14.3%) of 35 patients without baseline CMBs (**Figure 1**) and in 9 (64.3%) of 14 with CMBs detected in baseline MRI. Among a total of 66 new CMBs, 48 (72.7%) were localized in the cortical/subcortical area, 18 (27.3%) in deep brain structures, and 35 (53.0%) in the ipsilateral hemisphere. Hemorrhagic transformation (ECASS) was observed in 10 (20.4%) patients - 6 HI1, 2 HI2, 1 PH1, and 1 PH2. Baseline CMBs did not correlate significantly with hemorrhagic transformation ($p = 0.647$).

Patients with new CMBs were older (median 72.5, interquartile range (IQR) 66.5, 84.0 vs. 62.0, IQR 46.0, 75.5; $p = 0.026$), had higher creatinine level (median 1.0, IQR 0.9,1.1 vs. 0.8, IQR 0.7, 0.9; $p = 0.035$) and more often had higher counts of baseline CMBs: 9 (64.3%) vs. 5 (14.3%), $p < 0.001$. Other parameters were not statistically significantly different between the groups including pre-existing hypertension, the National Institutes of Health Stroke Scale (NIHSS) admission score, stroke subtype according to TOAST classification, the severity of leukoaraiosis, and baseline DWI lesion volume.

Multiple logistic regression analysis (**Table 6**) indicated that presence of baseline CMBs (risk ratio 5.95, 95% confidence interval CI 2.69–13.20, $p < 0.001$) and lower platelets level (risk ratio 0.992, 95% CI 0.986–0.998, $p = 0.007$) were independently associated with new CMBs.

DISCUSSION

In our patient sample, administration of rtPA resulted in the appearance of new CMBs in nearly 30% of the subjects with AIS, and the baseline CMBs were associated with the higher risk of the new ones appearing after the treatment. However, in this cohort, the baseline CMB load was not related to the increased risk of hemorrhagic transformation, unlike in many of the previous reports (21, 23, 32, 39). This finding seems not to be in line with the pathophysiological connections of CMBs and various vascular pathologies, notably small vessel disease, which in turn is related to increased vascular vulnerability and thus with hemorrhagic transformation—these correlations have been extensively discussed elsewhere (21–23). The reason for this discrepancy might be that these associations may be influenced by many confounding factors connected with the individual characteristics of a patient. CMBs are to be found in "healthy" populations, however, the insight in the available reports prove susceptibility of these populations for numerous future health risks that are additionally modulated by many coexisting factors such as hypertension, smoking, Apo E homozygosity, aspirin intake, white matter lesions or cerebral amyloid angiopathy (40). In addition, it has been reported that the correlation between CMBs and hemorrhagic transformation is not linear and that

TABLE 5 | Inter-observer agreement for the MRI assessment of CMBs.

CMBs on MRI	Baseline [kappa]*	Follow-up [kappa]*
Deep structures	0.64	0.78
Cortical/subcortical	0.58	0.74
All	0.63	0.77

** interobserver agreement was evaluated using the weighted Cohen's kappa with linear weights and interpreted in the following way: 0.01–0.20 as poor agreement, 0.21–0.40 as fair agreement, 0.41–0.60 as moderate agreement, 0.61–0.80 as substantial agreement, and above 0.80 as almost perfect agreement. The interobserver agreement was evaluated between the assessments of the neurologist (BJ) and the radiology team (ES and DO).*

TABLE 6 | Multiple logistic regression analysis for new CMBs in the follow-up T2*-EPI.

	New CMBs in the follow up T2*-EPI		
Risk factors	Adjusted risk ratio	95% CI	*p*-value
Presence of baseline CMBs	5.95	2.69–13.20	<0.001
Hypertension	5.45	0.99–29.90	0.051
Platelets	0.992	0.986–0.998	0.007
Observations	49		

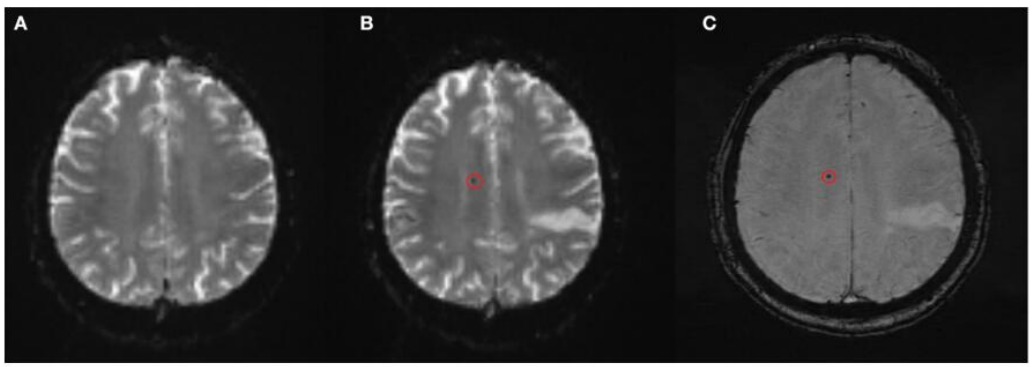

FIGURE 1 | New CMB found on the follow-up MRI on day 7–9 after rtPA treatment **(A)** baseline T2*-weighted EPI-GRE sequence, **(B)** follow-up T2*-weighted EPI-GRE, **(C)** susceptibility-weighted imaging confirmatory slice.

there is a threshold of baseline CMBs that, only when exceeded, results in higher risks for the transformation, especially for the sICH. The most commonly reported threshold is the > 10 CMBs (41) and the definite majority of our patients presented with not more than 3 baseline CMBs.

One of the future health issues of patients with CMBs is cognitive decline. The available studies suggest strong correlations between CMBs and cognitive impairment (15, 16). The substantial correlation between rtPA treatment and new CMBs found in our study, may have a major implication for the cognitive health of patients with AIS, and thus, longitudinal long-term studies in rt-PA treated patients with AIS are warranted for the need of powerful assessment of potential relations between thrombolytic treatment, CMBs, and cognitive function. This seems to be specifically important in patients with minor and/or lacunar stroke, where thrombolytic treatment does not have that much scientific data, as large vessel occlusion strokes, to prove favorable outcomes (42).

The study was not controlled with a placebo sample and therefore the direct correlation of new CMBs with rtPA treatment cannot be concluded. Additionally, the acute cerebral infarction itself is suggested to promote the development of CMBs (43). However, taking into account other studies on CMBs in acute stroke, and the known rate of the hemorrhagic infarction unrelated to rtPA administration, it is unlikely that this burden value would be as high as about 30% with no connection to rtPA. Furthermore, a strong indication of rtPA-CMBs correlation has been presented in the recent study by Miwa et al., where new CMBs were found only in patients who received rtPA (31). The high percentage of new CMBs in our study is much higher in comparison with other studies that revealed rates in the range of 4–13% (27–31). We believe that it is probably connected with a small sample size that resulted in incidental recruitment of more predisposed patients, as we discussed earlier.

This study has several methodological limitations. Importantly, as discussed earlier, we do not have a control group of non-thrombolysis patients to compare with. Another limitation of this study was the use of a 1.5-T field MR machine which is inferior to a 3-T in detecting CMBs, and the T2*EPI-GRE imaging sequence—much shorter but less sensitive than SWI for CMBs detection (44, 45). To support the lower sensitivity of T2*EPI-GRE sequences, SWI sequences were additionally used to confirm the CMB assessments. Finally, our study encompassed a relatively small sample of subjects, which is, however, similar to many of the reported cohorts. The main reason for the small number of patients is the conflict of interest between the optimal timing of rtPA treatment and the demanding circumstances of MRI testing that is necessary for proper CMBs assessment.

In conclusion, in this study, we present that baseline CMBs burden in patients with AIS is associated with a higher risk of new CMBs after rtPA treatment, but not with the risk of hemorrhagic transformation. New CMBs alone or combined with other selected characteristics (e.g., age, platelet count, or creatine level as indicated in this study) may become a useful predictor of long-term CMBs-related complications of thrombolytic treatment of stroke.

DATA AVAILABILITY STATEMENT

The original contributions presented in the study are included in the article, further inquiries can be directed to the corresponding author.

ETHICS STATEMENT

The studies involving human participants were reviewed and approved by the Independent Bioethics Committee for Scientific Research at Medical University of Gdańsk, Poland (Approval No. NKBBN/76/19). The participants provided their written informed consent to participate in this study. Written informed consent was obtained from the individuals for the publication of any potentially identifiable images or data included in this article.

AUTHOR CONTRIBUTIONS

BJ co-conceptualization of the study, patient recruitment, data assessment and analysis, combined analysis of all data, and writing. AG-G patient recruitment, data assessment and analysis, writing, and editing. DO neuroimaging data collection and assessment and writing. ES neuroimaging data assessment. AW statistical analysis and writing. BR clinical data assessment. BK conceptualization and funding receipt (a major project), writing, review, editing, and coordination. All authors contributed to the article and approved the submitted version.

FUNDING

Neuroimaging data were part of our project funded by Siemens Heathineers (research grant for the Medical University of Gdansk, PI – BK, 2018; Contract Number C00229230). The authors declare that this study received funding from Siemens Heathineers. The funder was not involved in the study design, collection, analysis, interpretation of data, the writing of this article or the decision to submit it for publication.

ACKNOWLEDGMENTS

This was a fully independent (–university-designed) project granted from the commercial institution, following the extensive review process. All the procedures within the study were carried out by independent academic researchers and clinicians.

REFERENCES

1. Emberson J, Lees KR, Lyden P, Blackwell L, Albers G, Bluhmki E, et al. Effect of treatment delay, age, and stroke severity on the effects of intravenous thrombolysis with alteplase for acute ischaemic stroke: a meta-analysis of individual patient data from randomised trials. *Lancet.* (2014) 384:1929–35. doi: 10.1016/S0140-6736(14)60584-5
2. Hacke W, Kaste M, Bluhmki E, Brozman M, Dávalos A, Guidetti D, et al. Thrombolysis with alteplase 3 to 4.5 hours after acute ischemic stroke. *N Engl J Med.* (2008) 359:1317–29. doi: 10.1056/NEJMoa0804656

3. Thomalla G, Simonsen CZ, Boutitie F, Andersen G, Berthezene Y, Cheng B, et al. MRI-guided thrombolysis for stroke with unknown time of onset. *N Engl J Med.* (2018) 379:611–22. doi: 10.1056/NEJMoa1804355
4. Thomalla G, Boutitie F, Ma H, Koga M, Ringleb P, Schwamm LH, et al. Intravenous alteplase for stroke with unknown time of onset guided by advanced imaging: systematic review and meta-analysis of individual patient data. *Lancet.* (2020) 396:1574–84. doi: 10.1016/S0140-6736(20)32163-2
5. Campbell BCV, Ma H, Ringleb PA, Parsons MW, Churilov L, Bendszus M, et al. Extending thrombolysis to 4·5-9 h and wake-up stroke using perfusion imaging: a systematic review and meta-analysis of individual patient data. *Lancet.* (2019) 394:139–47. doi: 10.1016/S0140-6736(19)31053-0
6. Larrue V, von Kummer R R, Müller A, Bluhmki E. Risk factors for severe hemorrhagic transformation in ischemic stroke patients treated with recombinant tissue plasminogen activator: a secondary analysis of the European-Australasian Acute Stroke Study (ECASS II). *Stroke.* (2001) 32:438–41. doi: 10.1161/01.STR.32.2.438
7. IST-3 collaborative group, Sandercock P, Wardlaw JM, Lindley RI, Dennis M, Cohen G, et al. The benefits and harms of intravenous thrombolysis with recombinant tissue plasminogen activator within 6 h of acute ischaemic stroke (the third international stroke trial [IST-3]): a randomised controlled trial. *Lancet.* (2012) 379:2352–63. doi: 10.1016/S0140-6736(12)60768-5
8. Karaszewski B, Houlden H, Smith EE, Markus HS, Charidimou A, Levi C, et al. What causes intracerebral bleeding after thrombolysis for acute ischaemic stroke? Recent insights into mechanisms and potential biomarkers. *J Neurol Neurosurg Psychiatry.* (2015) 86:1127–36. doi: 10.1136/jnnp-2014-309705
9. Whiteley WN, Emberson J, Lees KR, Blackwell L, Albers G, Bluhmki E, et al. Risk of intracerebral haemorrhage with alteplase after acute ischaemic stroke: a secondary analysis of an individual patient data meta-analysis. *Lancet Neurol.* (2016) 15:925–33. doi: 10.1016/S1474-4422(16)30076-X
10. Charidimou A, Werring D. Cerebral microbleeds: detection, mechanisms and clinical challenges. *Future Neurol.* (2011) 6:587–611. doi: 10.2217/fnl.11.42
11. Greenberg SM, Vernooij MW, Cordonnier C, Viswanathan A, Al-Shahi Salman R, Warach S, et al. Cerebral microbleeds: a guide to detection and interpretation. *Lancet Neurol.* (2009) 8:165–74. doi: 10.1016/S1474-4422(09)70013-4
12. Wardlaw JM, Smith EE, Biessels GJ, Cordonnier C, Fazekas F, Frayne R, et al. Neuroimaging standards for research into small vessel disease and its contribution to ageing and neurodegeneration. *Lancet Neurol.* (2013) 12:822–38. doi: 10.1016/S1474-4422(13)70124-8
13. Lee J, Sohn EH, Oh E, Lee AY. Characteristics of cerebral microbleeds. *Dement Neurocogn Disord.* (2018) 17:73–82. doi: 10.12779/dnd.2018.17.3.73
14. Poels MM, Vernooij MW, Ikram MA, Hofman A, Krestin GP, van der Lugt A, et al. Prevalence and risk factors of cerebral microbleeds: an update of the Rotterdam scan study. *Stroke.* (2010) 41:S103–6. doi: 10.1161/STROKEAHA.110.595181
15. Yatawara C, Guevarra AC, Ng KP, Chander R, Lam BYK, Wong A, et al. The role of cerebral microbleeds in the incidence of post-stroke dementia. *J Neurol Sci.* (2020) 412:116736. doi: 10.1016/j.jns.2020.116736
16. Paradise M, Seruga A, Crawford JD, Chaganti J, Thalamuthu A, Kochan NA, et al. The relationship of cerebral microbleeds to cognition and incident dementia in non-demented older individuals. *Brain Imaging Behav.* (2019) 13:750–761. doi: 10.1007/s11682-018-9883-3
17. Li L, Wu DH, Li HQ, Tan L, Xu W, Dong Q, et al. Association of cerebral microbleeds with cognitive decline: a longitudinal study. *J Alzheimers Dis.* (2020) 75:571–9. doi: 10.3233/JAD-191257
18. Nakamori M, Hosomi N, Tachiyama K, Kamimura T, Matsushima H, Hayashi Y, et al. Lobar microbleeds are associated with cognitive impairment in patients with lacunar infarction. *Sci Rep.* (2020) 10:16410. doi: 10.1038/s41598-020-73404-6
19. Haller S, Bartsch A, Nguyen D, Rodriguez C, Emch J, Gold G, et al. Cerebral microhemorrhage and iron deposition in mild cognitive impairment: susceptibility-weighted MR imaging assessment. *Radiology.* (2010) 257:764–73. doi: 10.1148/radiol.10100612
20. Poels MM, Ikram MA, van der Lugt A, Hofman A, Niessen WJ, Krestin GP, et al. Cerebral microbleeds are associated with worse cognitive function: the Rotterdam Scan Study. *Neurology.* (2012) 78:326–33. doi: 10.1212/WNL.0b013e3182452928
21. Charidimou A, Shoamanesh A, Wilson D, Gang Q, Fox Z, Jäger HR, et al. Cerebral microbleeds and postthrombolysis intracerebral hemorrhage risk Updated meta-analysis. *Neurology.* (2015) 85:927–4. doi: 10.1212/WNL.0000000000001923
22. Wilson D, Charidimou A, Ambler G, Fox ZV, Gregoire S, Rayson P, et al. Recurrent stroke risk and cerebral microbleed burden in ischemic stroke and TIA: a meta-analysis. *Neurology.* (2016) 87:1501. doi: 10.1212/WNL.0000000000003183
23. Zand R, Tsivgoulis G, Singh M, McCormack M, Goyal N, Ishfaq MF, et al. Cerebral microbleeds and risk of intracerebral hemorrhage post intravenous thrombolysis. *J Stroke Cerebrovasc Dis.* (2017) 26:538–44. doi: 10.1016/j.jstrokecerebrovasdis.2016.11.127
24. Wilson D, Ambler G, Lee KJ, Lim JS, Shiozawa M, Koga M, et al. Cerebral microbleeds and stroke risk after ischaemic stroke or transient ischaemic attack: a pooled analysis of individual patient data from cohort studies. *Lancet Neurol.* (2019) 18:653–65. doi: 10.1016/S1474-4422(19)30197-8
25. Best JG, Ambler G, Wilson D, Lee KJ, Lim JS, Shiozawa M, et al. Development of imaging-based risk scores for prediction of intracranial haemorrhage and ischaemic stroke in patients taking antithrombotic therapy after ischaemic stroke or transient ischaemic attack: a pooled analysis of individual patient data from cohort studies. *Lancet Neurol.* (2021) 20:294–303. doi: 10.1016/S1474-4422(21)00024-7
26. Pisters R, Lane DA, Nieuwlaat R, de Vos CB, Crijns HJ, Lip GY, et al. novel user-friendly score (HAS-BLED) to assess 1-year risk of major bleeding in patients with atrial fibrillation: the Euro Heart Survey. *Chest.* (2010) 138:1093–100. doi: 10.1378/chest.10-0134
27. Jeon SB, Kwon SU, Cho AH, Yun SC, Kim JS, Kang DW. Rapid appearance of new cerebral microbleeds after acute ischemic stroke. *Neurology.* (2009) 73:1638–44. doi: 10.1212/WNL.0b013e3181bd110f
28. Kimura K, Aoki J, Shibazaki K, Saji N, Uemura J, Sakamoto Y. New appearance of extraischemic microbleeds on T2*-weighted magnetic resonance imaging 24 hours after tissue-type plasminogen activator administration. *Stroke.* (2013) 44:2776–81. doi: 10.1161/STROKEAHA.113.001778
29. Yan S, Chen Y, Zhang X, Liebeskind DS, Lou M. New microbleeds after thrombolysis: contiguous thin-slice 3T MRI. *Medicine.* (2014) 93:e99. doi: 10.1097/MD.0000000000000099
30. Braemswig TB, Villringer K, Turc G, Erdur H, Fiebach JB, Audebert HJ, et al. Predictors of new remote cerebral microbleeds after IV thrombolysis for ischemic stroke. *Neurology.* (2019) 92:e630–8. doi: 10.1212/WNL.0000000000006915
31. Miwa K, Koga M, Inoue M, Yoshimura S, Sasaki M, Yakushiji Y, et al. Cerebral microbleeds development after stroke thrombolysis: A secondary analysis of the THAWS randomized clinical trial. *Int J Stroke.* (2021) 3:17474930211035023. doi: 10.1177/17474930211035023
32. Capuana ML, Lorenzano S, Caselli MC, Paciaroni M, Toni D. Hemorrhagic risk after intravenous thrombolysis for ischemic stroke in patients with cerebral microbleeds and white matter disease. *Neurol Sci.* (2021) 42:1969–76. doi: 10.1007/s10072-020-04720-y
33. Powers WJ, Rabinstein AA, Ackerson T, Adeoye OM, Bambakidis NC, et al. Guidelines for the Early Management of Patients With Acute Ischemic Stroke: 2019 Update to the 2018 Guidelines for the Early Management of Acute Ischemic Stroke: A Guideline for Healthcare Professionals From the American Heart Association/American Stroke Association. *Stroke.* (2019) 50:e344–e418 doi: 10.1161/STR.0000000000000211
34. Rapalino O, Heberlein M, Heberlein K. New strategies for protocol optimization for clinical MRI : rapid examinations and improved patient care. *Siemens Magnetom.* (2016) 2:22–25.
35. Prakkamakul S, Witzel T, Huang S, Boulter D, Borja MJ, Schaefer P, et al. Ultrafast brain MRI: clinical deployment and comparison to conventional brain MRI at 3T. *J Neuroimaging.* (2016) 26:503–10. doi: 10.1111/jon.12365
36. Fazekas F, Chawluk JB, Alavi A, Hurtig HI, Zimmerman RA. MR signal abnormalities at 1.5 T in Alzheimer's dementia and normal aging. *AJR Am J Roentgenol.* (1987) 149:351–6. doi: 10.2214/ajr.149.2.351
37. Wahlgren N, Ahmed N, Dávalos A, Ford GA, Grond M, Hacke W, et al. Thrombolysis with alteplase for acute ischaemic stroke in the Safe Implementation of Thrombolysis in Stroke-Monitoring Study (SITS-MOST): an observational study. *Lancet.* (2007) 369:275–82. doi: 10.1016/S0140-6736(07)60149-4

38. Adams HP, Bendixen BH, Kappelle LJ, Biller J, Love BB, Gordon DL, et al. Classification of subtype of acute ischemic stroke. Definitions for use in a multicenter clinical trial. TOAST. Trial of Org 10172 in Acute Stroke Treatment. *Stroke.* (1993) 24:35–41. doi: 10.1161/01.STR.24.1.35
39. Charidimou A, Turc G, Oppenheim C, Yan S, Scheitz JF, Erdur H, et al. Microbleeds, cerebral hemorrhage, and functional outcome after stroke thrombolysis. *Stroke.* (2017) 48:2084–90. doi: 10.1161/STROKEAHA.116.012992
40. Das AS, Regenhardt RW, Vernooij MW, Blacker D, Charidimou A, Viswanathan A. Asymptomatic cerebral small vessel disease: insights from population-based studies. *J Stroke.* (2019) 21:121–38. doi: 10.5853/jos.2018.03608
41. Chen J, Duris K, Yang X. Effect of cerebral microbleeds on hemorrhagic transformation and functional prognosis after intravenous thrombolysis of cerebral infarction. *Brain Hemorrhages.* (2021). doi: 10.1016/j.hest.2021.05.004
42. Karaszewski B, Wyszomirski A, Jabłoński B, Werring DJ, Tomaka D. Efficacy and safety of intravenous rtPA in ischemic strokes due to small-vessel occlusion: systematic review and meta-analysis. *Transl Stroke Res.* (2021) 12:406–15. doi: 10.1007/s12975-021-00890-9
43. Charidimou A, Kakar P, Fox Z, Werring DJ. Cerebral microbleeds and recurrent stroke risk: systematic review and meta-analysis of prospective ischemic stroke and transient ischemic attack cohorts. *Stroke.* (2013) 44:995–1001. doi: 10.1161/STROKEAHA.111.000038
44. Cheng AL, Batool S, McCreary CR, Lauzon ML, Frayne R, Goyal M, et al. Susceptibility-weighted imaging is more reliable than T2*-weighted gradient-recalled echo MRI for detecting microbleeds. *Stroke.* (2013) 44:2782–6. doi: 10.1161/STROKEAHA.113.002267
45. Kaaouana T, Bertrand A, Ouamer F, Law-Ye B, Pyatigorskaya N, Bouyahia A, et al. Improved cerebral microbleeds detection using their magnetic signature on T2*-phase-contrast: a comparison study in a clinical setting. *Neuroimage Clin.* (2016) 15:274–83. doi: 10.1016/j.nicl.2016.08.005

Conflict of Interest: The authors declare that the research was conducted in the absence of any commercial or financial relationships that could be construed as a potential conflict of interest.

Publisher's Note: All claims expressed in this article are solely those of the authors and do not necessarily represent those of their affiliated organizations, or those of the publisher, the editors and the reviewers. Any product that may be evaluated in this article, or claim that may be made by its manufacturer, is not guaranteed or endorsed by the publisher.

scientific reports

Check for updates

OPEN

SWATH-MS for prospective identification of protein blood biomarkers of rtPA-associated intracranial hemorrhage in acute ischemic stroke: a pilot study

Bartosz Karaszewski[1]✉, Anna Gójska-Grymajło[1], Paulina Czaplewska[2], Bartosz Jabłoński[1], Aleksandra E. Lewandowska[2], Daria Ossowska[1], Adam Wyszomirski[1], Marek Hałas[1] & Edyta Szurowska[3]

Intravenous recombinant tissue plasminogen activator (rtPA) is, besides mechanical thrombectomy, the highest class evidence based reperfusion treatment of acute ischemic stroke (AIS). The biggest concern of the therapy is symptomatic intracranial hemorrhage (sICH), which occurs in 3–7% of all treated patients, and is associated with worse functional outcome. Finding a method of the powerful identification of patients at highest risk of sICH, in order to increase the percentage of stroke patients safely treated with rtPA, is one of the most important challenges in stroke research. To address this problem, we designed a complex project to identify blood, neuroimaging, and clinical biomarkers combined for prospective assessment of the risk of rtPA-associated ICH. In this paper we present results of blood proteomic and peptide analysis of pilot 41 AIS patients before rtPA administration (the test ICH group, n = 9 or the controls, without ICH, n = 32). We demonstrated that pre-treatment blood profiles of 15 proteins differ depending on whether the patients develop rtPA-associated ICH or not. SWATH-MS quantification of serum or plasma proteins might allow for robust selection of blood biomarkers to increase the prospective assessment of rtPA-associated ICH over that based solely on clinical and neuroimaging characteristics.

Acute stroke, with ischemic stroke comprising 80% of all cerebrovascular incidents, has been recognized as one of the core problems in clinical medicine in need of prevention and treatment. It remains one of the most deleterious diseases that produce high social and economic costs worldwide. In 2016, of the 17.8 million deaths due to cardiovascular disease worldwide, 5.7 million were due to strokes[1]. In 2013, there were almost 25.7 million stroke survivors globally (71% with ischemic stroke) and 113 million disability adjusted life years due to stroke (58% due to ischemic stroke)[2].

Introduction of acute reperfusion treatment: intravenous thrombolysis, and in the past 5 years—the mechanical thrombectomy, in combination with specific and general stroke unit procedures, have greatly improved functional outcome after ischemic stroke. Thrombolytic treatment with recombinant tissue plasminogen activator (rtPA) was the first breakthrough in the reperfusion, thus in some sense causative, stroke treatment. Intravenous rtPA is the mainstay and the highest class evidence based method of acute ischemic stroke treatment, and is currently recommended 0–4.5 h after stroke onset[3]. Moreover, some patients selected with dedicated neuroimaging and special clinical characteristics might be treated even beyond the standard time window[4].

In most patients decision on i.v. rtPA administration is straightforward, however, in some cases it might be complex. The biggest concern is the symptomatic intracranial hemorrhage (sICH), which occurs in 3–7% of all treated patients, and is associated with worse 90-day functional outcome and higher disability than in those untreated[3,5]. There are various measures to quantify the extension of rtPA-associated ICH in clinical trials including the European Cooperative Acute Stroke Study (ECASS) scale (Table 1). Clinical measures used to

[1]Department of Adult Neurology, Medical University of Gdańsk & University Clinical Center, Gdańsk, Poland. [2]Intercollegiate Faculty of Biotechnology UG&MUG, University of Gdańsk, Gdańsk, PL, Poland. [3]II Department of Radiology, Medical University of Gdańsk, Gdańsk, Poland. ✉email: bartosz@karaszewski.org

Hemorrhage classification	Radiographic appearance
Hemorrhage infarction type 1 (HI1)	Small hyperdense petechiae
Hemorrhage infarction type 2 (HI2)	More confluent hyperdensity throughout the infarct zone; without mass effect
Parenchymal hematoma type 1 (PH1)	Homogeneous hyperdensity occupying < 30% of the infarct zone; some mass effect
Parenchymal hematoma type 2 (PH2)	Homogeneous hyperdensity occupying > 30% of the infarct zone; significant mass effect. Or, any homogenous hyperdensity located beyond the borders of the infarct zone

Table 1. The European Cooperative Acute Stroke Study scale of the hemorrhagic transformation after the thrombolytic treatment[43,44].

quantify the neurological deterioration due to rtPA-related sICH include SITS-MOST (The Safe Implementation of Thrombolysis in Stroke-Monitoring Study) and ECASS III[3]. The former is defined as intracerebral hemorrhage classified as local or remote PH2 within 24–36 h after rtPA bolus administration with the clinically important deterioration of neurological status, whereas the latter is defined as any hemorrhage with clinical deterioration of 4 or more points on the National Institutes of Health Stroke Scale (NIHSS) score.

Meta-analysis of nine trials of intravenous rtPA administration versus control[6] showed increased risk of PH2 [6.8% vs 1.3%, OR 5.55 (4.01–7.70)]. SITS-MOST registry also revealed higher frequency of PH2 [3.7% vs 0.6%, OR 6.67 (4.11–10.84)] and fatal intracerebral hemorrhage [2.7% vs 0.4%, OR 7.14 (3.98–12.79)].

Apart from the most common intraparenchymal hemorrhages anatomically related to ischemic lesion, in some patients treatment with i.v. rtPA is complicated by bleeding located remotely from the lesion, which may constitute a substantial portion of all ICHs and affect as many as 27.5% of patients[7]. However, there is little information on the prevalence of the remote-ICHs from large clinical trials on rtPA therapy for stroke.

Finding a method of the powerful (highly specific and selective) identification of patients at highest risk of sICH, in order to increase the percentage of stroke patients safely treated with rtPA, is one of the most important challenges in stroke research. The SITS-MOST identified nine independent risk factors for sICH: baseline NIHSS score, serum glucose, systolic blood pressure, history of hypertension, age, body weight, stroke onset to treatment time, aspirin monotherapy, and dual antiplatelet therapy with aspirin and clopidogrel. Unfortunately, any patterns or combinations of these and other characteristics into scoring systems (GRASPS, Glucose, Race, Age, Sex, Pressure, Stroke Severity; DRAGON (Dense Artery, Rankin Score, Age, Glucose, Onset to Treatment Time, National Institutes of Health Stroke Scale (NIHSS)), SEDAN (Sugar, Early Infarct Signs, Dense Artery, Age, NIHSS)) still perform poorly and have only modest predictive value for identifying patients at risk[8].

To address this problem we designed a major and complex project to identify blood, neuroimaging, and clinical biomarkers combined for prospective assessment of the risk of intracranial hemorrhage (ICH) after thrombolytic treatment of acute ischemic stroke (Investigator Initiated Study funded from Siemens Healthineers, 2018, to B. Karaszewski, Medical University of Gdansk) with analysis of multiple-origin data with deep learning techniques (hypothesis-free approach). The study was designed to recruit 400 ischemic stroke patients treated with i.v. rtPA, but herein we present results of blood proteomic and peptide analysis of pilot 41 patients.

The proteomic approach has already been separately recognized as a valuable and comprehensive method enabling insights into the pathophysiology of stroke with proteomic profile assessed in the brain of stroke patients[9–12], in the endothelial progenitor cells[13], in platelets[14] or in thrombi-emboli retrieved during the mechanical thrombectomy[15]. In 2015, a proteomics chip study on large Swedish PIVUS and ULSAM cohorts proved ten proteins to be related to the incident of stroke[16]. In another study on H-type hypertension related stroke, with use of iTRAQ-based LC–MS/MS proteomics approach, AT-3, CRP, ApoB, and AHSG were proved to be the strongest predictors of this type of stroke[17]. The same iTRAQ-based LC–MS approach was used in 50 stroke patients and 60 proteins showed a ≈1.5-fold change, with candidate proteins vWF, ADAMTS13, S100A7, and DLG4 confirmed through ELISA to corroborate with the experimental findings[18]. In the two phase SpecTRA study using liquid chromatography/multiple reaction monitoring-mass spectrometry, insulin-like growth factor-binding protein 3 and serum paraoxonase/lactonase 3 were found to be reliable and reproducible biomarkers for TIA in the Emergency Department settings[19]. In another study on TIA/minor stroke, ceruloplasmin, complement component C8 gamma (C8γ), and platelet basic protein were significantly different between the ischemic group (TIA and minor stroke) and the controls[20] Finally, the SWATH method was used for analysis of serum of 20 ischemic stroke patients and 11 proteins were defined as candidate biomarkers[21].

There are only two proteomic studies that concern rtPA treatment in ischemic stroke. In one of them plasma from acute stroke patients was analyzed pre- and post-intravenous tPA using tandem mass spectrometry and protein array profiling. The rtPA treated patients presented with distinct and elongated degradomic patterns in comparison to non-tPA treated patients[22]. In the second study, high-resolution mass spectrometry and long high-performance liquid chromatography were used to investigate changes in blood proteins after stroke and as a result of thrombolysis treatment. In this study ten patients were treated with rtPA and had up to 5 blood samples collected at different time points after stroke with 26 proteins being proved to be expressed differently and 23 proteins showing significant changes of expression over time[23]. However, up to date there have been no proteomic studies specifically confronting the possible biomarkers of hemorrhagic complications in stroke patients treated with rtPA, which make the release of the partial patient sample data reasonable. Due to its small size, and assumed biomolecular character of this paper, we do not here combine all individual data (clinical, neuroimaging, proteomic) into the scoring systems. Herein, we reveal our general methodological approach with shortlisting of blood peptide or protein candidates selected with Sequential Window Acquisition of All

	Without ICH (N = 32)	With ICH (N = 9)	*p* value*
NIHSS on admission			0.221
Min–Max	1.00–18.00	2.00–17.00	
Mean	6.12	7.78	
Median (Q1,Q3)	5.00 (3.00, 6.25)	7.00 (4.00, 11.00)	
NIHSS on discharge			0.458
Min–Max	0.00–15.00	0.00–7.00	
Mean	1.44	2.22	
Median (Q1,Q3)	0.50 (0.00, 1.25)	1.00 (0.00, 3.00)	
Age			0.344
Min–Max	19.00–94.00	51.00–91.00	
Mean	64.56	72.56	
Median (Q1,Q3)	67.00 (52.00, 80.25)	71.00 (59.00, 84.00)	
Sex, male	11 (34.4%)	6 (66.7%)	0.128
Hypertension	23 (71.9%)	8 (88.9%)	0.410
Diabetes	8 (25.0%)	3 (33.3%)	0.680
Hiperlipidemia	20 (62.5%)	8 (88.9%)	0.228
Atrial Fibrillation	7 (21.9%)	0 (0.0%)	0.315
Active smoking	10 (31.2%)	3 (33.3%)	< 1.000
Baseline infarct volume [ml]			0.050
Min–Max	0.00–64.02	1.14–55.57	
Mean	11.88	23.87	
Median (Q1,Q3)	2.63 (0.00, 17.02)	16.02 (10.36, 36.91)	

Table 2. Basic clinical and neuroimaging characteristics of ischemic stroke patients with and without intracranial hemorrhage after rtPA treatment. ICH—intracranial hemorrhage, NIHSS—National Institute of Health Stroke Scale; Q1—the first quartile; Q3—the third quartile; *Mann–Whitney U test was applied for comparison of quantitative data, whereas Fisher's exact test was used to compare binomial data; *p* value equal or less than 0.05 was considered statistically significant.

Theoretical Mass Spectra (SWATH-MS) that in the future might increase sensitivity and selectivity of the rtPA-associated sICH risk calculations.

There are obviously plenty other studies aiming at identifying serum or plasma prognostic biomarkers of rtPA-related hemorrhagic transformation in patients with acute ischemic stroke. However, in general they are based on far different methodological, technical and analytical approach to that described in this paper, and the selected biomarker—candidates have been characterized by relatively low sensitivity or selectivity thus so far not being applicable for clinical practice, and need further investigations[24–33].

Results

Careful visual assessment of the initial neuroimaging data revealed a DWI hyperintensive lesion corresponding with neurological deficit in 30 out of 41 patients (73%). The ICH was found in 9 cases on the 5–9 day follow up SWI and T2* MR Imaging. In this initial phase of the study we did not differentiate ICH into symptomatic and asymptomatic. However, the clinical status and neuroimaging characteristics of each individual participant are listed in the Supplementary Table 1. The summary of the clinical and neuroimaging characteristics of the participants divided into two groups—with and without ICH are presented in Table 2.

We have identified 261 proteins at 1% FDR in a joint database search of unfractionated and fractionated plasma and serum pool samples of ischemic stroke patients (Supplementary Tables 2, 2a and 2b). In the case of 237 of these, 2 or more confidently recognized peptides were detected. With the use of this database search as a spectral library for SWATH-MS analysis of clinical samples, 180 proteins could be reliably quantified in a relative manner. DIA measurements of plasma and serum samples were processed simultaneously, and obtained results were divided into two sets of data prior to the statistical analysis.

Patients were assigned to the test group (i.e.with ICH, n = 9) and the control group (without ICH, n = 32) resulting in two experimental datasets subjected to statistical analysis by Mann–Whitney U tests. Any changes in protein concentrations with p value < 0.05 were considered significant, no matter the extent of the concentration change. In all investigated statistical comparisons, we detected 15 differential proteins (Table 3) in both analyzed fluids. Eight of them were found in serum as specific to this biological fluid, (2 proteins present at higher concentrations and 6 proteins present at lower concentrations in the test group). Immunoglobulin heavy constant gamma 4 was present at the most increased concentrations in the test group (about 3.6-fold) and thyroxine-binding globulin was present at the most decreased concentrations (almost 0.6-fold). In case of plasma, 7 proteins were present at different concentrations with p value < 0.05. All seven proteins were present at higher concentrations in the test group with immunoglobulin heavy variable 5–51 demonstrating highest increase (more than 1.7-fold). Notably, fibrinogen beta and gamma chains were present in this group with 1.3-fold increase.

Uniprot ID	Protein name	Serum		Plasma	
		p value*	Fold change†	*p* value*	Fold change†
Q96PD5	N-acetylmuramoyl-L-alanine amidase	**0.005**	**0.804**	0.115	1.138
P08697	Alpha-2-antiplasmin	**0.008**	**0.616**	0.614	0.935
P02768	Serum albumin	**0.009**	**1.372**	0.682	1.038
P05543	Thyroxine-binding-globulin	**0.011**	**0.598**	0.592	1.158
P02790	Hemopexin	**0.015**	**0.676**	0.614	0.994
P01861	Immunoglobulin heavy constant gamma 4	**0.024**	**3.618**	0.950	1.056
P01019	Angiotensinogen	**0.037**	**0.747**	0.508	0.980
P02749	Beta-2-glycoprotein 1	**0.044**	**0.718**	0.413	1.118
P04278	Sex hormone-binding globulin	0.889	1.002	**0.006**	**1.483**
P02675	Fibrinogen beta chain	0.313	0.760	**0.017**	**1.377**
P02679	Fibrinogen gamma chain	0.164	0.765	**0.021**	**1.230**
A0A0C4DH38	Immunoglobulin heavy variable-5–51	0.999	1.106	**0.021**	**1.779**
Q06033	Inter-alpha-trypsin inhibitor heavy chain H3	0.297	0.852	**0.025**	**1.213**
P02649	Apolipoprotein E	0.487	1.105	**0.027**	**1.532**
P36955	Pigment epithelium-derived factor	0.651	0.909	**0.038**	**1.270**

Table 3. Serum and plasma protein candidates for biomarkers related to the intracranial hemorrhage after rtPA treatment in ischemic stroke patients. †The fold change represents the change of protein concentration between the patients with and without ICH, *Any changes in protein concentrations with p value < 0.05 were considered significant, no matter the extent of the concentration change.

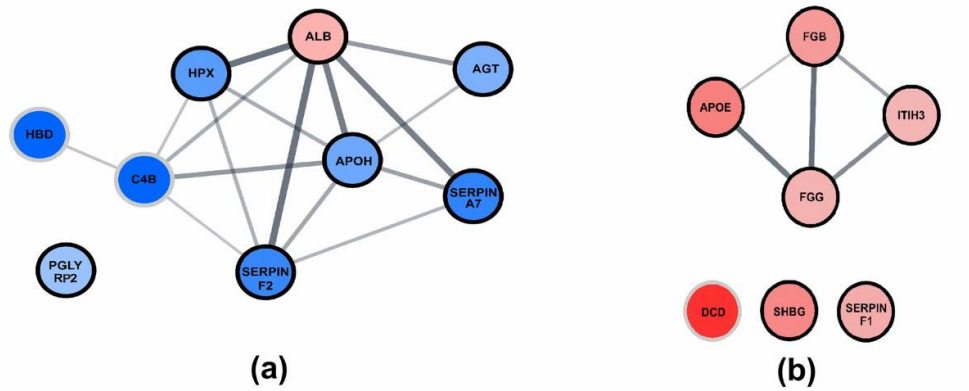

Figure 1. The Cytoscape visualization of STRING-generated network composed of experimentally verified protein–protein interactions among the quantified proteins (**a**) for serum and (**b**) for plasma. Nodes with a bold edge correspond to proteins with statistically significant change between the groups (p value < 0.05), whereas nodes with grey edges correspond to proteins with a verified interaction with those proteins and at least twofold concentration change between the groups, which was however insignificant (p value > 0.05). The gradation of the fill corresponds to the value of the concentration fold changes, the darker the greater the change, shades of red and blue correspond to increased and decreased concentration in the test group, respectively.

To get a more thorough look at the proteomic landscape of our patients with ICH, we constructed interaction networks in Cytoscape software and conducted basic functional enrichment analysis. In these networks, we included also the proteins with at least twofold concentration change, which interacted well with those described previously (Fig. 1). The network constructed for serum was based on 7 differentiators recognized by STRING database, with 6 proteins forming the network along with 2 additional proteins. We conducted functional enrichment analysis on constructed network in terms of GO Process, which yielded terms associated with regulation of response to stress and to external stimulus (APOH, HPX, SERPINF2, PGLYRP2, AGT, C4B), negative regulation of endopeptidase activity (SERPINF2, SERPINA7, AGT, C4B), and regulation of blood vessel diameter by renin-angiotensin (SERPINF2, AGT). Moreover, top three Reactome Pathways terms were: response to elevated platelet cytosolic Ca^{2+}, platelet degranulation (APOH, ALB, SERPINF2), and scavenging of heme from plasma (HPX, ALB). The network for plasma was based on 6 differentiating proteins, out of which 4 interacted only with each other. Dermcidin, present at more than twofold higher concentration in the test group, was added to

the network. Primarily enriched GO Processes included: negative regulation of response to external stimulus (APOE, SERPINF1, FGB, FGG), negative regulation of blood coagulation and regulation of blood vessel diameter (APOE, FGB, FGG). The main enriched Reactome pathways consisted of: integrin signaling, platelet aggregation (FGB, FGG), and response to elevated platelet cytosolic Ca^{2+} (FGB, FGG, ITIH3).

Discussion

In this pilot study we demonstrate that pre-treatment blood proteomic profiles of ischemic stroke patients differ depending on whether the patients develop rtPA-associated ICH or not. SWATH-MS quantification of plasma and serum proteins might allow for robust selection of blood biomarkers to increase the prospective assessment of rtPA-associated ICH, and it is likely that these parameters will strengthen assessments of the brain bleeding risk over that based solely on clinical and neuroimaging characteristics.

Taking a small sample analyzed for this paper, any major pathophysiological conclusions related to individual compounds might be too speculative. Moreover, due to the same reason, we did not analyze these pilot data with the main endpoint division of patients i.e. into those with symptomatic versus asymptomatic ICH, working on any versus non-ICH instead. These limitations must be taken into account in interpreting these results, whereas the portion of the pathophysiological discussion below might be only treated as selective and exemplary.

Ning et al. found that rtPA treated patients have distinct degradomic pattern from those untreated at the early (< 24 h post-tPA) phase[22]. Their analysis of the individual degradomic fractions revealed degradation of fibrinogen and alpha 2 macroglobulin, which are thrombolysis pathway-related proteins. They were able to identify different components of fibrinogen subunits in the post-thrombolytic profiles (alpha and gamma subunits). Our data reveal increase (about 1.3-fold) of the fibrinogen beta and gamma chain in rtPA-associated ICH, in comparison with non-ICH patients, which might be partially consistent with the former despite different design of both studies with pre- versus post-thrombolysis blood sample analyses. Although the latter do not allow for direct comparisons of our report with Dagonnier et al., it is worth noting that this study also indicated substantial changes in fibrinogen serum concentrations during the first 24 h after stroke[23].

SWATH, the proteomic analysis used in this study, allows only to determine the trend of changes, not the actual protein concentration, but its sensitivity and selectivity is sufficient to distinguish between patient groups according to the endpoint characteristics. Moreover, the micro LC system with QT of spectrometer seems a reasonable solution for clinical studies even in emergency settings because, compared to nano LC systems, the time of analysis is significantly reduced from hours to several dozen minutes and may be even shorter with future technical developments. It also provides the ability to maintain a high throughput in opposition to nano systems, which makes it possible to test a large number of samples in a relatively short time with low operator intervention in maintaining the system in continuous operation.

Rapid and comprehensive clinical assessment is crucial to improve functional outcome and reduce mortality. Stroke centers, in order to ensure short door-to-needle time, use CT scan as a basic neuroimaging modality in acute ischemic stroke prior to rtPA administration. In our study, we applied baseline MRI, with "GO-Brain", fast, early phase, stroke-dedicated, Siemens-designed protocol that comprises only necessary sequences and lasts only a few minutes more than regular head CT. Nevertheless, this protocol imposes considerable pressure on stroke neurologists, nurses, paramedics and radiologists, that need to act even faster in order to prepare patients for the rtPA treatment in the shortest possible time. The brisk and efficient cooperation of emergency department staff is indispensable to complete essential steps in qualification process—blood samples collection and brain MRI scan prior to rtPA administration, but also in the follow-up phase 7–9 days after the incident of stroke. Altogether, this challenging and unique approach represents major asset of the project and adds additional value to its results.

This project aims at selection of molecular, neuroimaging and clinical parameters combined to mathematically support pre-treatment estimation of the risk of rtPA-associated ICH. Development of a new tool for selection of patients at risk will eventually require 'big data' analysis (350–400 patients, multiple parameters of various origin for each) with deep learning techniques. However, in this paper, based on a pilot patient sample and analyzed with simple statistical approach, we only demonstrate that information on selected blood protein and peptide concentrations might potentially increase the power of the risk-calculation engine over that based solely on clinical and neuroimaging characteristics. In our analysis, the results of statistical calculations do not contain *p* values adjustment for multiple testing; we prespecified and designed this pilot study to show and discuss a special, hypothesis free approach in clinical medicine, whereas the original portion of this study is primarily exploratory, with no intention to confirm the usefulness of any biomarker pattern at this stage of the major project.

Materials

Study population and blood collection. All study participants were acute ischemic stroke patients hospitalized at the Stroke Unit of the Department of Adult Neurology, University Clinical Center, Medical University of Gdansk, Poland, between March 20, 2019 and February 20, 2020.

During the pilot recruitment period we performed 94-MRI examinations in patients with suspected acute stroke. It is worth noting that—to avoid any treatment delays—we used only a rapid MR protocol that includes only a few sequences necessary to gain neuroimaging information on potential contraindications to systemic thrombolysis (the "GoBrain" application). Fifty-six patients received i.v. rtPA treatment according to standard inclusion and exclusion criteria based on major management guidelines. The only additional inclusion criterion was lack of contraindication to MRI. All patients underwent MRI and blood sampling prior to the treatment, and on day 7–9 from stroke onset. Following this, we have excluded 15 patients due to lack- or poor quality of follow-up neuroimaging data or lack of follow-up blood sample. 41 patients entered the final analysis.

For the initial (pilot) phase of the study, we enrolled 41 patients. The study was approved by the local ethics committee: The Independent Bioethics Committee for Scientific Research at the Medical University of Gdańsk,

Poland. All research procedures were performed in accordance with the principles of the World Medical Association Declaration of Helsinki. All the patients provided informed consent for the involvement in the study. Comprehensive clinical data on the study group was gathered. The summary clinical and neuroimaging characteristics of the participants are presented in Table 2. The clinical status and neuroimaging characteristics of each individual participant are listed in the Supplementary Table 1.

Peripheral venous blood samples were collected on admission, just before the rtPA treatment. Each patient had two blood samples collected—a EDTA-coated tube to acquire plasma and one with silica clot activator to obtain serum (Becton Dickinson Vacutainer). Shortly after collection samples were cetrifuged, serum and plasma were transferred to Eppendorf tubes and were safely stored in deep-freeze (− 80 °C). The collection of serum and plasma samples was then sent to the Intercollegiate Faculty of Biotechnology of University of Gdansk and Medical University of Gdansk, Poland, for proteomic analysis.

Neuroimaging studies. All study participants had MRI scan on admission and a non-contrast CT scan the next day (day 2) after the rtPA treatment. Additionally, 39 patients had MRI scan on day 5–9 after admission.

All MRI examinations were performed using 1.5T Siemens Magnetom Aera system. First MRI examination was performed using fast "GO-Brain" protocol composed of the following sequences: sagittal T1 weighted, axial diffusion-weighted imaging (DWI) (b value 0 and 800), and ADC maps, axial T2 weighted fluid attenuation inversion recovery (FLAIR) and axial T2* weighted. The second MRI protocol included the same sequences as the initial MRI, together with additional sequences: axial diffusion tensor imaging (DTI), axial susceptibility-weighted imaging (SWI), three-dimensional axial T1 weighted, and sagittal T2 weighted sequences.

The short MRI protocol sequences including DWI with ADC maps, and FLAIR were assessed by an experienced radiologist.Volumes of the lesions corresponding to acute ischemia were calculated based on visual assessments of their expansion using the software (syngo.via) integrated with the machine console (see Supplementary Table 1).

The ICH presence and expansion was assessed with 5–9 day SWI and T2*-weighted MR Imaging. In cases where follow up MRI scan wasn't available (2 patients) the assessment was based on the routine post-rtPA follow-up CT scan (see Supplementary Table 1).

Proteomics. *Protein fractionation for spectral library preparation.* Pool samples of serum and plasma were fractionated prior proteolytic digestion to enrich the spectral library employed in SWATH-MS quantification. Three strategies were applied: (i) ultrafiltration, (ii) immunodepletion, and (iii) protein enrichment. Ultrafiltration was conducted using Amicon filters (Merck) with membranes of 30 kDa and 100 kDa molecular weight cutoff. Both retentate and filtrate fractions were analyzed. Immunodepletion involved application of the Multiple Affinity Removal Spin Cartridge Human 14 (MARS-14) kit (Agilent Technologies, Santa Clara, CA) according to manufacturer's protocol. Besides the isolated low abundant protein fractions, the bound high abundant protein fractions were also further processed for MS measurements. Protein enrichment was carried out with the ProteoMiner kit (BioRad) according to the manufacturer's protocol.

All serum and plasma samples were prepared for proteomic analysis according to standard Filter Aided Sample Preparation (FASP) procedure[34]. 50 µl of the sample was mixed with 200 µl of the solution containing 1% SDS, 100 mM Tris/HCl pH 8, 50 mM DTT (lysis solution) and incubated at 95 °C for 10 min. First, the protein concentration was established for each sample by measuring absorbance at 280 nm (MultiskanTM Thermo) using the µDrop plate. For each digestion in triplicate, 100 µg of proteins were added to 200 ml of 8 M urea in 0.1 M Tris/HCl pH 8.5 (UA solution) placed in the 10 kDa microcons (Merck) and centrifuged at 10,000×*g* for 30 min. Washing and centrifuging steps with UA were repeated 3 times for samples were protein concentration was higher than 10 mg/ml; in the case of lower content, two additional washing steps with UA were added. Next, 100 µl of 55 mM iodoacetamide (IAA) solution in UA was added, and samples were kept in the dark for 20 min. After centrifugation, alkylated proteins were washed on the membrane three times with 100 µl of UA solution and two times with 100 µl of 50 mM Tris HCl pH 8.5 buffer (DB). Finally, the microcones were placed in new tubes, and a solution containing 2 µg of trypsin was added to each sample. The digestion was performed overnight at 37 °C in the incubation chamber. Tryptic peptides were collected after centrifugation at 10,000×*g* for 20 min. Each membrane was additionally washed with 125 and 100 µl of DB solution. Before the final clean-up, the peptide concentration was measured. Generated tryptic peptides were desalted with StageTips according to the protocol described by Rappsilber et al.[35]. For each desalting step, 10 µg of the peptides was taken and desalted on StageTip containing three layers of 3 M Empore C18 exchange disks. Peptides eluated by 100 µl 60% acetonitrile/1% acetic acid were concentrated to 20 µl prior to MS analysis.

Liquid chromatography and mass spectrometry. LC–MS/MS analysis was performed with the use of a Triple TOF 5600 + mass spectrometer (SCIEX Framingham, MA) coupled with the Ekspert MicroLC 200 Plus System (Eksigent, Redwood City, CA, USA). All chromatographic separations were performed on the ChromXP C18CL column (3 µm, 120 Å, 150 × 0.3 mm). The chromatographic gradient for each MS run was 8–40% B (solvent A 0% aqueous solution 0.1% formic acid, solvent B 100% acetonitrile 0.1% formic acid) in 30 min. The whole system was controlled by the SCIEX Analyst TF 1.7.1 software. Measurements for spectral library were acquired in triplicate. Each cycle of applied DDA method comprised of precursor spectra accumulation in 250 ms in the range of 400–100 m/z followed by top 20 precursor's product ion spectra accumulation in 100 ms in the range of 100–1500 mz, resulting in a total cycle time of 2.3 s. Formerly fragmented precursor ions were dynamically excluded.

SWATH mass spectrometry. Experiments on clinical samples were performed in a looped product ion mode with the spectrometer set to high sensitivity focus. A set of 25 transmission windows of variable width was constructed with the use of SwathTUNER software based on equalized frequency of precursor ions and covered the precursor mass range of 400–1000 m/z[36]. The collision energy for each window was calculated for + 2 to + 5 charged ions centered upon the window with a spread of five. The SWATH-MS survey scan was acquired in the range covered by constructed windows in the beginning of each cycle with the accumulation time of 50 ms, and following SWATH-MS/MS spectra product ion scans were collected in the range of 100 to 1500 m/z in 40 ms, which resulted in the total cycle time of 1.1 s.

Data analysis. Database search was performed with ProteinPilot 4.5 software (Sciex) using the Paragon algorithm against the SwisProt Homo sapiens database (version from 8.04.20, 20 350 entries) with an automated false discovery rate, and standard parameters (alkylation of cysteine residues by iodoacetamide, digestion by trypsin, ID focus on biological modifications).

Next, a spectral library was created with the group file data processing in PeakView v. 2.2 (SCIEX), with settings as described in detail by Lewandowska et al.[37–39]. Joint search for library generation included unfractionated pool samples and samples fractionated as described in "Protein fractionation for spectral library preparation" paragraph, both serum and plasma. Files from SWATH experiments for each sample were downloaded to PeakView software and processed with the previously established library. Resulting data were exported to the .xml file and exported to Marker View software. All data were normalized using total area sums (TAS) approach. The mass spectrometry proteomics data have been deposited to the ProteomeXchange Consortium via the PRIDE partner repository with the dataset identifier PXD021713[40]. Cytoscape 3.8.0[41] and STRING 11.0[42] were used for the interactome network visualization.

Statistical analysis. Continuous variables were described as medians and the first and third quartiles. The technical variability of the quantitative proteomics was calculated using the quartile coefficient of dispersion. Categorical data was presented as frequencies and percentages. We applied the Mann–Whitney U test for comparison of quantitative variables between unpaired two samples of patients—with and without ICH, whereas the Fisher exact test was used to compare binomial data. The 2-tailed tests were carried out at a significance level of $p \leq 0.05$. All statistical analyses were performed using the R statistical package (version 3.6.3; https://www.r-project.org/).

Conclusions

This study is the first to show pre-treatment characteristics of blood protein profiles for haemorrhagic complications related to intravenous administration of rtPA in acute ischemic stroke patients.

However, the biomarker list will require confirmation with a larger sample (in course) and in other populations of stroke patients. This project aims at section of new parameters to mathematically support pre-treatment estimation of the risk of rtPA-associated ICH but further considerations of biological roles and relations between the selected biomarkers might be also of special interest.

The main general target of this paper is to indicate an extensive significance of combined mathematical analysis of data (or big data) of different origin (proteomic, other "omic", demographic, clinical, imaging-neuroimaging, environmental) in clinical medicine to generate tools that might support individual therapeutic decisions throughout precise calculation of probability of various outcome scenarios.

Received: 18 November 2020; Accepted: 27 August 2021
Published online: 21 September 2021

References

1. Global Health Estimates 2016: Deaths by cause, age, sex, by country and by region, 2000–2016. Geneva, World Health Organization (2018).
2. Feigin, V. L. *et al.* Update on the global burden of ischemic and hemorrhagic stroke in 1990–2013: The GBD 2013 study. *Neuroepidemiology* **45**, 161–176 (2015).
3. Hacke, W. *et al.* Thrombolysis with alteplase 3 to 4.5 hours after acute ischemic stroke. *N. Engl. J. Med.* **359**, 1317–1329 (2008).
4. Campbell, B. C. V. *et al.* Ischaemic stroke. *Nat. Rev. Dis. Prim.* **5**, 70 (2019).
5. Sandercock, P. *et al.* The benefits and harms of intravenous thrombolysis with recombinant tissue plasminogen activator within 6 h of acute ischaemic stroke (the third international stroke trial [IST-3]): A randomised controlled trial. *Lancet* **379**, 2352–2363 (2012).
6. Whiteley, W. N. *et al.* Risk of intracerebral haemorrhage with alteplase after acute ischaemic stroke: A secondary analysis of an individual patient data meta-analysis. *Lancet Neurol.* **15**, 925–933 (2016).
7. Strbian, D. *et al.* Patient outcomes from symptomatic intracerebral hemorrhage after stroke thrombolysis. *Neurology* **77**, 341–348 (2011).
8. Karaszewski, B. *et al.* What causes intracerebral bleeding after thrombolysis for acute ischaemic stroke? Recent insights into mechanisms and potential biomarkers. *J. Neurol. Neurosurg. Psychiatry* **86**, 1127–1136 (2015).
9. Cuadrado, E. *et al.* The proteome of human brain after ischemic stroke. *J. Neuropathol. Exp. Neurol.* **69**, 1105–1115 (2010).
10. Datta, A., Akatsu, H., Heese, K. & Sze, S. K. Quantitative clinical proteomic study of autopsied human infarcted brain specimens to elucidate the deregulated pathways in ischemic stroke pathology. *J. Proteomics* **91**, 556–568 (2013).
11. Dayon, L. *et al.* Brain extracellular fluid protein changes in acute stroke patients. *J. Proteome Res.* **10**, 1043–1051 (2011).
12. Ning, M. *et al.* Proteomic temporal profile of human brain endothelium after oxidative stress. *Stroke* **42**, 37–43 (2011).
13. Brea, D. *et al.* Proteomic analysis shows differential protein expression in endothelial progenitor cells between healthy subjects and ischemic stroke patients. *Neurol. Res.* **33**, 1057–1063 (2011).
14. Cevik, O., Baykal, A. T. & Sener, A. Platelets proteomic profiles of acute ischemic stroke patients. *PLoS ONE* **11**, e0158287 (2016).

15. Rao, N. M. *et al.* Peptide composition of stroke causing emboli correlate with serum Markers of atherosclerosis and inflammation. *Front. Neurol.* **8**, 427 (2017).
16. Lind, L. *et al.* Discovery of new risk markers for ischemic stroke using a novel targeted proteomics chip. *Stroke* **46**, 3340–3347 (2015).
17. Zhou, F. *et al.* Plasma proteomics reveals coagulation, inflammation, and metabolic shifts in H-type hypertension patients with and without acute ischemic stroke. *Oncotarget* **8**, 100384–100395 (2017).
18. Sharma, R. *et al.* Proteomic signature of endothelial dysfunction identified in the serum of acute ischemic stroke patients by the iTRAQ-based LC-MS approach. *J. Proteome Res.* **14**, 2466–2479 (2015).
19. Penn, A. M. *et al.* Verification of a proteomic biomarker panel to diagnose minor stroke and transient ischaemic attack: Phase 1 of SpecTRA, large scale translational study. *Biomarkers* **23**, 392–405 (2018).
20. George, P. M. *et al.* Novel TIA biomarkers identified by mass spectrometry-based proteomics. *Int. J. Stroke* **10**, 1204–1211 (2015).
21. Lee, J. *et al.* Proteomics-based identification of diagnostic biomarkers related to risk factors and pathogenesis of ischemic stroke. *Diagnostics* **10**, 340 (2020).
22. Ning, M. *et al.* Proteomic protease substrate profiling of tPA treatment in acute ischemic stroke patients: A step toward individualizing thrombolytic therapy at the bedside. *Transl. Stroke Res.* **1**, 268–275 (2010).
23. Dagonnier, M. *et al.* Discovery and longitudinal evaluation of candidate biomarkers for ischaemic stroke by mass spectrometry-based proteomics. *Biomark. Insights* **12**, 1177271917749216 (2017).
24. Cesari, M., Pahor, M. & Incalzi, R. A. Plasminogen activator inhibitor-1 (PAI-1): A key factor linking fibrinolysis and age-related subclinical and clinical conditions. *Cardiovasc. Ther.* **28**, e72–e91 (2010).
25. Yuan, R. *et al.* Predictive value of plasma matrix metalloproteinase-9 concentrations for spontaneous haemorrhagic transformation in patients with acute ischaemic stroke: A cohort study in Chinese patients. *J. Clin. Neurosci.* **58**, 108–112. https://doi.org/10.1016/j.jocn.2018.09.014 (2018).
26. Wang, W., Li, M., Chen, Q. & Wang, J. Hemorrhagic transformation after tissue plasminogen activator reperfusion therapy for ischemic stroke: Mechanisms, models, and biomarkers. *Mol. Neurobiol.* **52**(3), 1572–1579. https://doi.org/10.1007/s12035-014-8952-x (2015).
27. Lakhan, S. E., Kirchgessner, A., Tepper, D. & Leonard, A. Matrix metalloproteinases and blood–brain barrier disruption in acute ischemic stroke. *Front. Neurol.* **4**, 32 (2013).
28. Foerch, C. *et al.* Elevated serum S100B levels indicate a higher risk of hemorrhagic transformation after thrombolytic therapy in acute stroke. *Stroke* **38**(9), 2491–2495 (2007).
29. Ribo, M. M. J. *et al.* Admission fibrinolytic profile is associated with symptomatic hemorrhagic transformation in stroke patients treated with tissue plasminogen activator. *Stroke* **35**(9), 2123–2127 (2004).
30. Cocho, D. *et al.* Pretreatment hemostatic markers of symptomatic intracerebral hemorrhage in patients treated with tissue plasminogen activator. *Stroke* **37**(4), 996–999 (2006).
31. Wang, Y. *et al.* Association between non-high-density lipoprotein cholesterol and haemorrhagic transformation in patients with acute ischaemic stroke. *BMC Neurol.* **20**, 47. https://doi.org/10.1186/s12883-020-1615-9 (2020).
32. Strbian, D. *et al.* Symptomatic intracranial hemorrhage after stroke thrombolysis: the SEDAN score. *Ann. Neurol.* **71**, 634–641. https://doi.org/10.1002/ana.23546 (2012).
33. Kazmierski, R., Michalak, S., Wencel-Warot, A. & Nowinski, W. L. Serum tight-junction proteins predict hemorrhagic transformation in ischemic stroke patients. *Neurology* **79**, 1677–1685. https://doi.org/10.1212/WNL.0b013e31826e9a83 (2012).
34. Wiśniewski, J. R., Zougman, A., Nagaraj, N. & Mann, M. Universal sample preparation method for proteome analysis. *Nat. Methods* **6**, 359–362 (2009).
35. Rappsilber, J., Mann, M. & Ishihama, Y. Protocol for micro-purification, enrichment, pre-fractionation and storage of peptides for proteomics using StageTips. *Nat. Protoc.* **2**, 1896–1906 (2007).
36. Zhang, Y. *et al.* The use of variable Q1 isolation windows improves selectivity in LC–SWATH–MS acquisition. *J. Proteome Res.* **14**, 4359–4371 (2015).
37. Lewandowska, A. E. *et al.* Human follicular fluid proteomic and peptidomic composition quantitative studies by SWATH-MS methodology. Applicability of high pH RP-HPLC fractionation. *J. Proteomics* **191**, 131–142 (2019).
38. Ludwig, C. *et al.* Data-independent acquisition-based SWATH–MS for quantitative proteomics: A tutorial. *Mol. Syst. Biol.* **14**, e8126 (2018).
39. Gillet, L. C. *et al.* Targeted data extraction of the MS/MS spectra generated by data-independent acquisition: A new concept for consistent and accurate proteome analysis. *Mol. Cell. Proteomics* **11**, O111.016717 (2012).
40. Perez-Riverol, Y. *et al.* The PRIDE database and related tools and resources in 2019: Improving support for quantification data. *Nucleic Acids Res.* **47**, D442–D450 (2019).
41. Shannon, P. *et al.* Cytoscape: A software Environment for integrated models of biomolecular interaction networks. *Genome Res.* **13**, 2498–2504 (2003).
42. Szklarczyk, D. *et al.* STRING v11: Protein–protein association networks with increased coverage, supporting functional discovery in genome-wide experimental datasets. *Nucleic Acids Res.* **47**, D607–D613 (2019).
43. Hacke, W. *et al.* Intravenous thrombolysis with recombinant tissue plasminogen activator for acute hemispheric stroke: The European Cooperative Acute Stroke Study (ECASS). *JAMA J. Am. Med. Assoc.* **274**, 1017–1025 (1995).
44. Fiorelli, M. *et al.* Hemorrhagic transformation within 36 hours of a cerebral infarct: Relationships with early clinical deterioration and 3-month outcome in the European Cooperative Acute Stroke Study I (ECASS I) cohort. *Stroke* **30**, 2280–2284 (1999).

Acknowledgements

This investigator initiated and designed project is being funded by Siemens Helthineers (research grant for the Medical University of Gdansk, PI—Bartosz Karaszewski, 2018; Contract Number C00229230).

Author contributions

B.K.—conceptualization and main organization of the study, recruitment coordination and consultancy, data analysis coordination and piloting, writing (article concept with contents and flow design, review and editing), A.G.G., B.J.—patient recruitment, contribution to study organization and course, contribution to data analysis, management of biological samples and databases, writing (original draft preparation), P.C., A.L.—proteomic analysis, writing, D.O.—neuroimaging data collection and assessment, writing, A.W.—statistical analysis, writing, M.H.—patient recruitment; E.S.—neuroimaging data assessment.

Competing interests

This grant had been received from the commercial institution based on the review process of the university designed project. All procedures within this study were carried out by independent academic researchers and clinicians.

Additional information

Supplementary Information The online version contains supplementary material available at https://doi.org/10.1038/s41598-021-97710-9.

Correspondence and requests for materials should be addressed to B.K.

Reprints and permissions information is available at www.nature.com/reprints.

Publisher's note Springer Nature remains neutral with regard to jurisdictional claims in published maps and institutional affiliations.